Developing Metal-Selective Peptide Probes for the Extracellular Space

By

CHANTEL MAO
MASTER'S DEGREE - THESIS

Submitted in partial satisfaction of the requirements for the degree if

MASTER OF SCIENCE

in

Chemistry

in the

OFFICE OF GRADUATE STUDIES

of the

UNIVERSITY OF CALIFORNIA

DAVIS

Approved:

_____
Marie Heffern, Chair

_____
Alan Balch

_____
Randy Carney

Committee in Charge

2022

TABLE OF CONTENTS

ABSTRACT

Metals found in the human body are utilized to maintain normal functions such as cell proliferation, growth, and respiration.[1, 2] If trace amounts of metal ions in our body (approximately 10 μM) are not properly maintained, they have been shown to be involved in numerous diseases including cancer and degenerative diseases.[3–5] Although we understand that elevated levels of metals may be toxic and have delineating affects to our health, the mechanism behind metals in the body remain unknown due to the lack of tools we currently have to be able to selectively trace these metals in the extracellular space.

This thesis describes the strategies and challenges towards developing probes that are selective for metals in the extracellular space. Thus far, a peptide library was first built to discover potential Cu(II)-binding peptides. This peptide was then synthesized and conjugated to a fluorophore. Lastly, the Cu(II)- binding peptide was purified and subjected to cell-based assays to validate the utility of the peptide as a probe.

Unnatural amino acids have been shown to be more stable and targeted for metal binding when utilized for drug delivery or probes.[6] To further develop a potential Cu(II) selective probe, bipyridine-alanine unnatural amino acid was a good candidate to include for a future peptide library. Synthesis optimization for this unnatural amino acid are also discussed in this thesis.

Taking inspiration from my previous project for developing a Cu(II)-selective probe, oxytocin, a peptide hormone, has been studied to rely on metals in order to be recognized by the oxytocin receptor.[7] Since oxytocin is a cyclic peptide, reduced oxytocin (linear) analogs were designed and synthesized in hopes to be studied for Zn(II) mediated binding in order for

oxytocin receptor recognition. With fluorophore conjugation, it could then be investigated as a probe for Zn(II).

Altogether, the outcome of my thesis is to describe the approaches used thus far to develop peptide probes for monitoring copper and zinc in the extracellular space.

ACKNOWLEDGEMENTS

When I attended the Bioinorganic Conference at Caltech in 2018 as an undergraduate and met everyone in the Heffern lab (aside from Nate, who scared me when he tried to introduce himself to me**)**, I was definitely interested in applying and going to UC Davis. Three years later, here I am about to graduate from the Heffern lab.

Thank you, Marie, for literally being there for me since day one of my graduate school career. When I briefly met you at that conference, I was super interested in being your graduate student because of your passion for bioinorganic chemistry. Your drive and determination is infectious. You are such an inspiration to me, and I feel so grateful to have you as a mentor, not only in research, but just in life. Throughout my time in the lab, you've seen my struggles, pushed me to do better, and were just there for me, which I truly appreciate. Even though I had no idea what I was doing career-wise and even research- wise at time… and we've had many tough conversations… you've made me a strong, confident person that is ready to take on the world. Thank you for caring about me and my mental health too! Without your mentorship, I would have never known where my strengths lie and how to use them to my advantage. I will forever be grateful for everything you've taught me.

I would also like to thank Jess who I've grown so close to these past three years. Thank you for sticking by my side and advocating for me, when I was not bold enough to. Jess, thank you for laughing with me, having writing sessions with me, hunting triceratops with me, and going to see the sheepies (and felting) with me. I'll miss our tea time in the TC room. Thank you for teaching me UV-Vis, Western blots (yikes), and how to use the microscope and fix my cells! Both you and Estely have been sooo supportive and encouraging in my decisions and just me in general. I love how I can just go to you both for our venting sessions.

Estely, thank you for always checking in on me and my mental health, for our coffee dates, and being the best mentee I could've asked for. Thank you for instilling a confidence in myself that I didn't even know I had.. I literally don't know what I would do without you in graduate school! Seeing you from day 1 of graduate school until now, post-QE, I am so proud of you and all your accomplishments. You are such an inspiration to all those that are first-gen graduate students, including me! You are so selfless and courageous, and I love that so much about you. <3

Thank you, Nate, for literally being there for me since day 1 that I met you. While you did frighten me when I was an undergrad at the Bioinorganic conference, you clearly did not scare me away from the lab apparently. Thank you for always being so supportive of me and helping me learn cell culture (even when I was in denial) and step into the bio-world of our lab. The skills I gained from you are life changing. Thank you for your positive attitude in the lab and always encouraging me and boosting my confidence and just listening to me… I'm gonna miss rolling over to your lab space!

Alice, since day one I met you at visitation, you've been nothing but supportive throughout the whole time I've been in grad school. From all your baked goods and coffee breaks, to our weekly dinners, I don't know how I would've gotten this far without you. As we both wrap up our time here in Davis, I am so thankful to have a friend like you. You always said I was going to finish grad school before you, but we definitely did not see it ending like this… but now we all know it's definitely for the better (for both of us).

As for the rest of the lab, thank you for all the memories we've had! Sam, thank you for always checking in on me and being so relatable during my grad school career. I will miss seeing your head pop over the computer when I am at the LCMS. I'll also miss bothering you when I

couldn't figure out why random errors come up on the LCMS. JJ, thank you for your guidance and help when I first started out in the lab and had no idea what I was doing and literally taking time out of your day to help me and making sure I was okay when you saw I was in a mood. Vanessa, thank you for being so friendly to me ever since I joined the lab and asking me how I was doing! Shadowing you encouraged me to join the lab. Thanks for chatting with me and offering your help with UV-Vis when I was struggling so hard with that.

Without question, I also want to thank my family, especially my dad, mom, sister, grandma, and my grandpa.

Dad, thank you for working so hard all these years to give my sister and I a better life, and always encouraging us to do what we want to do and be happy with whatever we choose to do. All the nights that you worked literally 16 hour days for us to live comfortably are things I will always be grateful for. The advice you've given to me, I definitely took to heart, especially leading up to my decision to graduate with a Master's when I came to grad school to pursue a PhD. Thank you for reminding me to do what is best for me, and not let others judge me or their words affect me. Thank you for always thinking about me and calling me and talking to me!

Mom, thank you for always chatting with me and being there for me when I just needed someone to talk to. This thing called life isn't easy, and I am glad you are always listening. Your care for my sis and I cannot be described and I could not ask for another mom. Thank you for being so patient with me and supporting all my decisions and truly listening to my opinions from my perspective, even though we may not always agree. It takes a lot to do that, and I aspire to be just like that one day.

To my sis, Celine (aka Ming), thank you for always keeping me updated with the coolest trends, and offering me life advice… you're wiser beyond your years. You inspire me to choose

happiness and live a stress free life always. Although growing up we didn't always get along, I really appreciate the time that we do have together more these days. I love how you stand your ground and remind me to do the same. I also love how we text each other everyday, just about the most random things. Even though we are 330 miles away, you feel a lot closer to me than that.

To my grandma, thank you for taking care of my sis and I when we were little and spoiling us to our hearts content. It's only fitting now that my sis and I are spoiling you with what we can give you now. My heart is so full that you were able to visit me in Davis and explore the world with my family. I was so happy to see you happy and proud of everything I have accomplished so far. You remind me that even when I feel defeated, that it's just a little thing and that you are still always proud of my accomplishments. We've been through a lot this past year, but I am so inspired by your strength and independence. I only want to be like you someday.

Grandpa, this year has been so tough for all of us ever since you left us. I am so glad I got to see you one last time in January and documented the memories with pictures before you left this world peacefully. When I think of you, I just remember the times you took my sis and I out to eat pho and gave us money to play at the arcade, even though you did not have much money yourself or when you took my sis and I out to buy any of our favorite stationary pens, pencils, erasers, notebooks. I still remember the times you would pick up me and my sis from school in that Honda Element that my dad still kept as a reminder of you. When I look back at all the memories I have had with you, I think of how brave you were to take on your whole family and immigrated to the U.S. not knowing what was out there and what the future may hold… only knowing that you wanted to give your children a better life. You're the bravest man I know, even

up to your passing. Your perseverance throughout the past decade, especially is something I won't forget. After you left this earth, I got clarity with my decision of leaving with my Master's. I realized that all you wanted for everyone is to be happy together as a family and seeing them that way. You brought our family here so we can be happy and choose to live our lives how we want, which made me question why I was in grad school and if this program was as fulfilling as I thought it would be. Ever since then, I have extremely grateful to my family for supporting me with whatever decision I choose. I really miss you and wish you were here, but I know you are now in a better place.

Lastly, I would also like to thank Armin for sticking by me through it all. Grad school was never easy for me…. From those nights where I would cry and get frustrated with myself, research, and going through the QE, and now finishing off grad school with my Master's, job hunting, and prepping for interviews… you've seen me at my worst and still managed to help me get through those tough times. Even though you have a lot on your own plate, you still want to make sure that I'm okay and ensure that I wake up in a positive mood. When I am feeling discouraged and unhappy, you always know how to cheer me up! You have always supported me and encouraged me to believe in myself, even when I didn't and remind me to not undersell myself and my skills. Thank you for always listening to me vent, telling me that I can do this when I truly believe I couldn't, always pointing out that things are not as bad as they may seem to me (because I can be too dramatic), and just being my number one supporter in anything I do. Thank you for also being there for me and taking care of me as I wrapped up my time here. I'm excited for whatever may come in our future together.

CHAPTER 1: INTRODUCTION

1.1 Metal ions and diseases

First-row d-block metals like copper are important for our overall health and well-being[8]. These metal ions have been shown to be involved in numerous biochemical processes including respiration, growth, and cell proliferation[1]. However, dysregulation of metals have been associated with a variety of diseases including neurodegenerative diseases and cancer[1,9]. For example, accumulation of copper and zinc have been linked to neurodegenerative diseases including Alzheimer's disease and Wilson's disease[3] as well as in cancer.[9]

Despite the reported associations between elevated metal concentrations in diseases, we still do not fully understand how, why, and where these metals are involved in diseases due to the lack of tools to target metal ions in the extracellular space. Many tools that have been developed to study metal ions tend to focus on the intracellular space rather than the extracellular space. However to further understand the mechanism behind metal ions and their involvement in diseases, it is necessary to develop metal-selective tools for probing the extracellular space to improve and advance future therapeutics.

1.2 Current Approaches for Detecting Extracellular Copper

Copper, an abundant metal in biological systems, is necessary for normal functions in both the intra- and extracellular space including cellular signaling and mediating receptor-ligand binding.[3,5] It is present in its ionic form either tightly bound (static) or loosely bound (labile) to proteins.[3] The labile copper pool is believed to be important and associated with redox signaling and activity in the brain.[10,11] Our bodies are able to regulate and maintain copper levels by homeostasis due to copper being present in both the extracellular and intracellular environments

(Figure 1). In the extracellular space, labile pools are expected to be in the Cu(II) form due to the presence of dissolved O_2, whereas the intracellular labile pool is expected to be primarily in the Cu(I) state due to the high concentration of copper binding reductants like glutathione.[12] Due to its redox-active nature, biology must tightly regulate and maintain copper levels and oxidations states.[10] Disruption of this homeostasis may cause unwanted redox reactions and oxidative stress observed in disease states.[10]

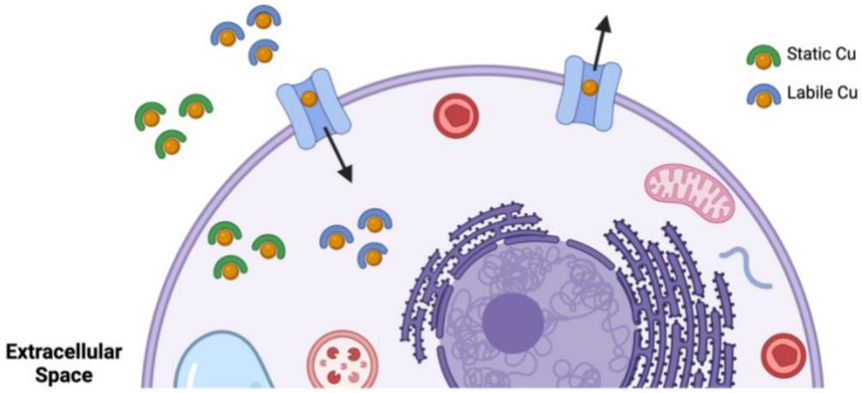

Figure 1. Static and labile copper pools in the extracellular space and intracellular space.

In addition to its levels and redox status, the localization of copper between the intracellular and extracellular space is important to its homeostasis. Utilizing X-ray fluorescence microscopy, Finney *et al* showed that excess copper can be translocated from the intra- to extracellular regions during angiogenesis.[13] However, further understanding of the mislocalization of copper and associated biological pathways is hampered by the lack of current methods to trace extracellular Cu(II).[13]

Current clinical standards either measure total copper levels in the blood or use indirect markers associated with copper.[12] Total copper levels are usually measured by Inductively Coupled Plasmon- Mass Spectrometry (ICP-MS). The most common clinical practice for assessing copper status, however, is by quantitation of ceruloplasmin, an abundant copper-

carrying protein in the serum.[14] While these methods are useful in extreme cases of copper dysregulation, it can yield inaccurate characterization of labile copper pools as it does not account for differences in copper redox states, binding environments, and spatial distribution.

To mitigate the complications that arise from measuring total copper pools, separative method have also been established. Solid Phase Extraction (SPE), is a method that can be used to separate between copper bound proteins from the non-copper bound proteins.[15] Protein adsorption can be accomplished by SPE using polyethylene (PE) material for different molecular weights.[16] Non-copper bound proteins are able to filter through the PE column and the desired protein is retained on the column and eluted. Therefore, being able to specifically measure exchangeable (labile) copper pools has been of interest for studying copper metabolism and use as a diagnostic tool.[15]

Another separative method applies chelators like ethylenediaminetetraacetic acid (EDTA) to isolate and quantify the exchangeable copper.[17] In this approach, EDTA is added to a serum sample to extract labile copper from the proteins they are abound to while leaving tightly-bound pools unaffected, then the mixture is separated by ultrafiltration.[16] Larger, complex proteins such as ceruloplasmin, serum albumin, and transcuprein or the tightly bound copper proteins are retained in the filter while, the labile copper, now bound to the small molecular-weight chelator are filtered through. The filtrate is then quantified by elemental analysis.[18] While this method has provided important insight into the general balance of static and labile pools, it suffers variability and inaccuracies due to the possibility that under certain conditions, the static pool may be chelated in part, leading to an overestimation of the labile copper pool.[18,19]

1.3 Current Approaches for Detecting Extracellular Zinc

Zinc is the second most abundant d-block metal ion in the body[20] and is involved in many key cellular processes including brain development and immunity[4,20]. Similar to copper, zinc exists as tightly bound or labile forms[21]. Both the excess or deficiency in Zn(II) intake as well as miscompartmentalization of the metal has been associated with a host of disorders, including Alzheimer's disease.[22] Tools for understanding Zn(II) fluctuations will help further elucidate its role and dynamics in both normal and pathological states.

Zinc is most frequently measured from blood plasma levels via mass spectrometry-basd elemental quantitation techniques.[20] However, reliable indicators for zinc status remain unavailable, requiring the use of indirect indicators. For instance, developmental indicators like stunting and anemia are considered suggestions of zinc dyshomeostasis, but with no corroborating molecular markers.[23] Given the indirect nature of these methods, they can only hint at, but not validate zinc imbalances. While molecular imaging tools have been developed towards the specific monitoring of Zn(II) fluxes *in vivo*, these tools either suffer from poor sensitivity or non-specific localization.[21,23–27]

Current tools for Zn(II) monitoring provide a broad picture of zinc status, but does not account for the localization of zinc. Therefore, developing a Zn(II) selective probe to monitor Zn(II) in real time in the extracellular space is necessary for a better understanding of Zn(II) and its relationship in diseases.

1.4 Scope of Thesis

This thesis describes the development of molecular imaging platforms geared towards understanding the role of metal dynamics in diseases. In order to accomplish this goal, the described work focuses on the development and validation of peptide probes to be selective for

Cu(II) in the extracellular space. In expanding this research to other metal ions, peptides were also designed to target extracellular Zn(II).

Chapter 2 discusses the development of peptide-based libraries to discover platforms for imaging extracellular Cu(II). Taking inspiration from sequence motifs of known metal-binding sites copper-coordinating residues were incorporated into a library of peptides derivatized from integrin-binding peptides. The general approach aimed at having integrin-binding only in the presence of Cu(II)-binding. Peptides were screened for their ability to bind to integrin-expressing cells only in the presence of Cu(II).

Learning from the candidates from the library screen in Chapter 2, Chapter 3, tests and derivatizes the "hits". Peptides were synthesized, labeled with a fluorescent dye, and purified. After successful isolation of the desired peptides, they were evaluated for their Cu(II)-binding abilities and assessed with cell-based assays for their potential as Cu(II)-selective peptide probes.

In an effort to expand the possible sequences for peptide libraries targeted to metal-binding, Chapter 4 describes the synthesis of non-natural amino acid building block, an Fmoc-protected bipyridine. Bipyridines are well-known to coordinate Cu(II) with high affinity.[28,29] The chapter includes the design of the synthetic route, and the optimization and conversion improvements for the first two steps of this multi-step synthesis.

In Chapter 5, the development of peptide probes for metal selectivity expanded to Zn(II) by building off of the peptide hormone, oxytocin. Oxytocin has been shown to interact with metals in a way that affects its binding towards its cognate receptor.[7] As oxytocin is naturally a cyclic peptide, we aimed to utilize its linear form (reduced oxytocin) to allow for Zn(II)-mediated conformational changes in a way that affects receptor recognition. This chapter

encompasses the design of reduced oxytocin and its analog, including the incorporation of a fluorescent dye.

Taken together, this thesis provides a launching point for peptide-based metal-selective probes for the extracellular space. The success of these projects will provide tools for scientists to have a better understanding of the role metals may play in diseases.

CHAPTER 2: DESIGN AND SCREEN OF A PEPTIDE LIBRARY FOR A COPPER(II)-SELECTIVE PROBE PLATFORM

2.1 Introduction

Copper plays an important role in normal physiological processes. At adequate concentrations, living organisms use copper in order to maintain vital processes including cell signaling, maintaining the integrity of blood vessels, and may participate in the modulation of receptor-ligand interactions.[3] On the other hand, abnormally high levels of copper are harmful,[3,15] being implicated in disorders such as Alzheimer's Disease and cancer.[3] While the correlation between elevated levels of copper and diseases has been documented, we do not fully understand the mechanism behind copper's involvement in these diseases due to the lack of tools to monitor and track copper in the extracellular space. Current tools provide powerful information on total copper levels and their changes diseases,[5,12] but to fully understand copper and its interactions in diseases states, targeted probes for extracellular Cu(II) are essential to improve future therapeutics.

This chapter discusses the efforts toward designing a Cu(II) selective probe using a peptide library screen with a specific goal of targeting the extracellular pool. The design of the library are first described followed by the cell-based screenings and validation of Cu(II-mediated peptide binding. Ultimately, once a Cu(II)-selective peptide is discovered from the peptide library, it may be further developed into a probe by incorporation of a signaling molecule such as a fluorophore as shown in Scheme 1.

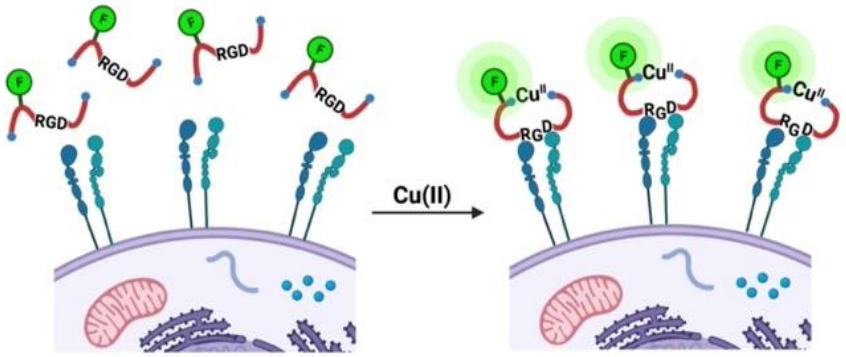

Scheme 1: General schematic of Cu(II)-sensing probe (fluorophore in green) localized on the cell surface via integrins. Linear peptides conformationally change then bind to integrins only in the presence of Cu(II) at the N- and C- terminus (blue dots). An increase in fluorescence can then be observed.

2.2 Design of the Peptide Library

To develop potential copper responsive peptide probes for detecting bioavailable copper, probe localization and selectivity were first considered. While several probes have been reported for imaging intracellular copper, the analogous tools for extracellular copper have been challenging to develop due to its redox activity, the dilute nature of the extracellular space, and the concentration dynamics throughout various regions in the body. We aimed to develop a peptide platform for a probe that could be 1) localized extracellularly but accumulate at a target point at the cell membrane for signal amplification and 2) selectively respond to Cu(II) over Cu(I) as well as other metal ions.

To target localization to the extracellular space, we elected to generate peptides that could bind extracellular receptors called integrins, but only in the presence of Cu(II). Integrins are overexpressed in many cell types and is involved in angiogenesis and tumor growth similarly to copper dyshomeostasis[30], making these cell surface receptors an ideal dock for our peptide probe. These cell surface receptors are involved in cell-cell and cell-extracellular matrix interaction and various biological processes including cell proliferation, migration, cell adhesion,

and apoptosis.[30–32] In particular, integrin $\alpha_v\beta_3$ is a receptor known to bind to various extracellular ligands.[32] In its cyclic form, $\alpha_v\beta_3$ integrin recognizes the motif, Arg-Gly-Asp (RGD). The RGD motif is considered the minimal integrin recognition for many extracellular matrix proteins and has been extensively studied and optimized for utility as a potential therapeutic.

The Lam lab at UC Davis developed and optimized the synthesis of a cyclic peptide that binds to the $\alpha_v\beta_3$ integrin with high affinity, termed the LXW64 cyclic peptide[32]. The binding of LXW64 peptide has the sequence containing the aforementioned RGD motif, cGRGDdc, where c= D-cysteine, d= D-napthalene, with a disulfide bridge formed from the D-Cys at the N- and C-terminus (Figure 1). Optimization studies found the D- amino acids, instead of the natural L-amino acids important for increasing stability of the peptide to enzymatic degradation[30,32] and validated the necessity for the RGD within a cyclized system for integrin recognition and binding to the cell surface. We thus designed a peptide library built on sequences containing the RGD motif.

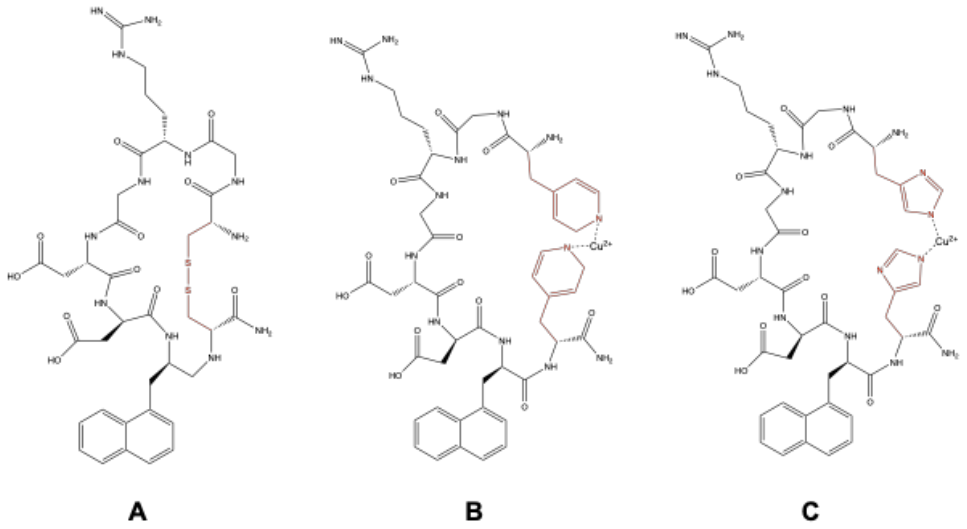

Figure 2. A) LXW64 cyclic peptide B) Pyr-2 peptide and C) His-2 peptide with copper-induced cyclization highlighted in red.

To bias the library towards Cu(II)-selectivity, we modified the LXW64 cyclic peptide to instead be linear and preclude initial recognition by the integrin. In this design, replacing the disulfide bond from D-cysteines in LXW64 (Figure 2A) with metal-coordinating amino acids (Figure 2B/C) would potentially allow for copper-mediated conformational changes. We hypothesized that Cu(II) binding would provide a cyclic-like conformation to the peptide to allow for integrin recognition via the RGD motif. The peptide library was thus built with the general sequence, X_1GRGDdGX_2, where X_1 and X_2 represent amino acids with copper-coordinating potential such as pyridine (Pyr), histidine (H). Meanwhile, Lysine (K), Aspartic Acid (D), Glutamic Acid (E), Ornithine (Orn), and Diaminopropanoic acid (Dpr) amino acids were also integrated into the general sequence as these amino acids have been shown to participate in Cu(II) interactions in non-classical binding motifs.[33] To obtain and test the various combinations on this sequence, the one-bead-one compound method (OBOC, Ch. 2.3) was utilized for high-throughput synthesis and screening for Cu(II)-selective peptides.

2.3 Applying the One-Bead-One- Compound Method for Cu(II) Binding Peptide Discovery

As described above, 7 amino acids (Pyr, H, K, D, E, Orn, Dpr) were chosen to be incorporated into the linear sequence, X_1GRGDdGX_2 at the N- and C- terminus (X_1 and X_2). OBOC was implemented to synthesize multiple, randomized peptides efficiently, with one sequence presenting on the surface of bead. The OBOC method, developed by the Lam Lab is an advantageous combinatorial approach for building a peptide library because 1) the split-and-pool method (Figure 3) allows for peptide variation in large quantities and 2) the beads can be separated when randomization is necessary and pooled together when the amino acids contain a shared motif, and 3) screening for positive hits on-bead is high throughput.[34]

To generate a peptide library, first, the resin is swollen and split into three filter columns (Figure 3). Then, the desired amino acids (A, B, C) are added in each columns and is coupled onto the resin. To keep the sequence randomized, the three columns are mixed together in one large column and split again into three filtered columns in order to randomize the second amino acid coupling. As shown, this would generate 9 different dipeptides. The split/mix approach continues until the desired peptide sequence is achieved. After successful synthesis of the peptide library, it is then subjected to the desired screening conditions.

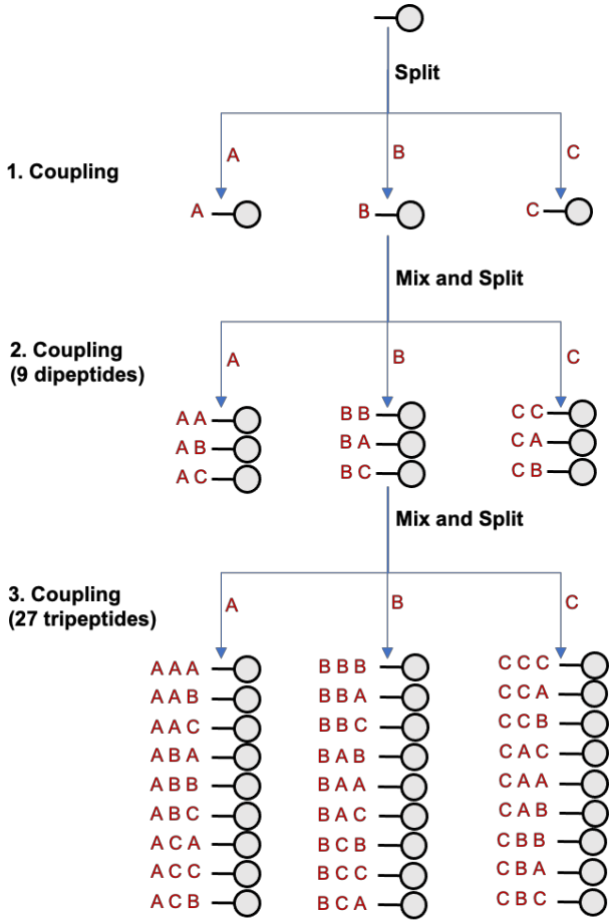

Figure 3. General split/mix synthesis approach to generate OBOC combinatorial library.

After generating the peptide library, the on-bead peptides can be subjected to a cell-based assay to identify sequences that exhibited the behavior of interest, which in our case is Cu(II)-dependent binding to the integrin receptor. The general screening process is as follows: the beads are plated in a 6-well plates and treated with the analyte of interest as needed (e.g. Cu(II)). After washing the wells of excess and unbound analyte, a cell line with the target receptor (e.g. integrin) is added to the beads to allow for binding. Beads that are surrounded by the cells are defined as a positive hit. The beads can be reused in order to screen multiple controls or additional analytes.

Once positive hits are identified, Edman degradation is used to identify the sequences of the hits. Edman degradation was developed by Pehr Edman in 1950, and has been one of the primary ways to sequence unknown peptide sequences[35]. This method involves the peptide of interest to be reacted with phenyl isothiocyanate (PITC) at the N-terminus of a peptide (Figure 4). With this chemical reaction, each amino acid is subsequently removed at each degradation by reacting with phenyl isothiocyanate (PITC), where the sequence can be determined using the Edman degradation sequencer[35,36]. The elution times of each degradation of the peptide are then compared with the standards of expected elution times for each amino acid in order for the sequence to be determined.

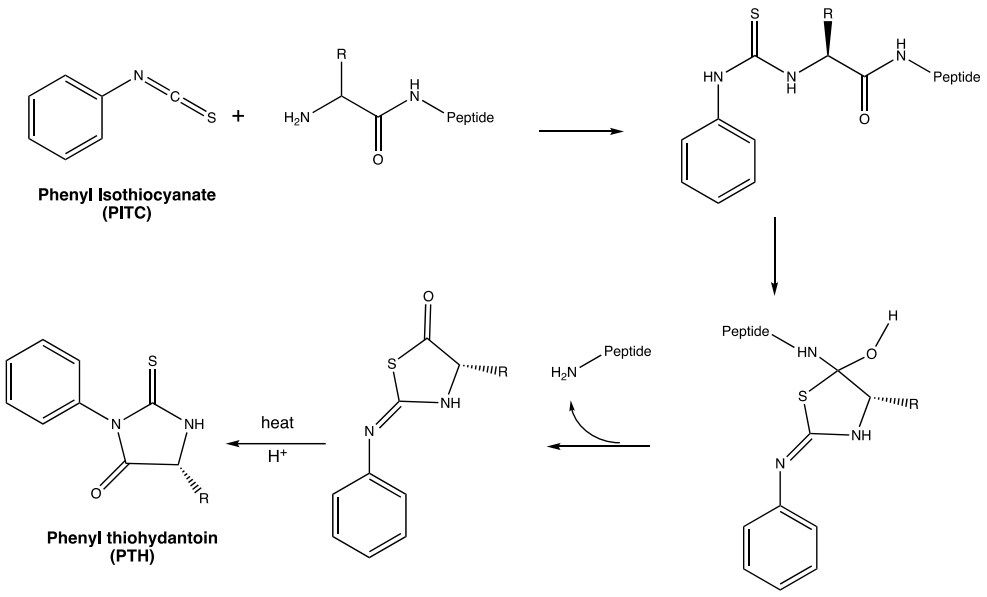

Figure 4. Reaction for Edman degradation sequencing[37]

2.4 Results and Discussion

After synthesizing the target peptide library on-bead via OBOC method, the beads were plated and used to discover Cu(II) binding peptides. First, Cu(II) was incubated with the plated beads for 30 minutes to allow for peptide binding. Then U87 cells, which overexpress the integrin of interest, were added and allowed to incubate for 30 minutes. The beads were subsequently imaged to assess cellular binding. The peptides were similarly screened with other including Zn(II), Fe(II), Mg(II), Ca(II), K(I), Na(I) to help identify and exclude non-selective metal interactions. The images were analyzed to identify hits in the form of beads surrounded by cells. Each image that was used for Cu(II) screening was overlayed with the images from the screen with other metals to eliminate non-selective hits. Beads that came out as hits for both Cu(II) and the other metals were classified as "false positives". On the other hand, a bead surrounded by cells in only the Cu(II) screening was defined as a true Cu(II) hit for further analysis (Figure 5).

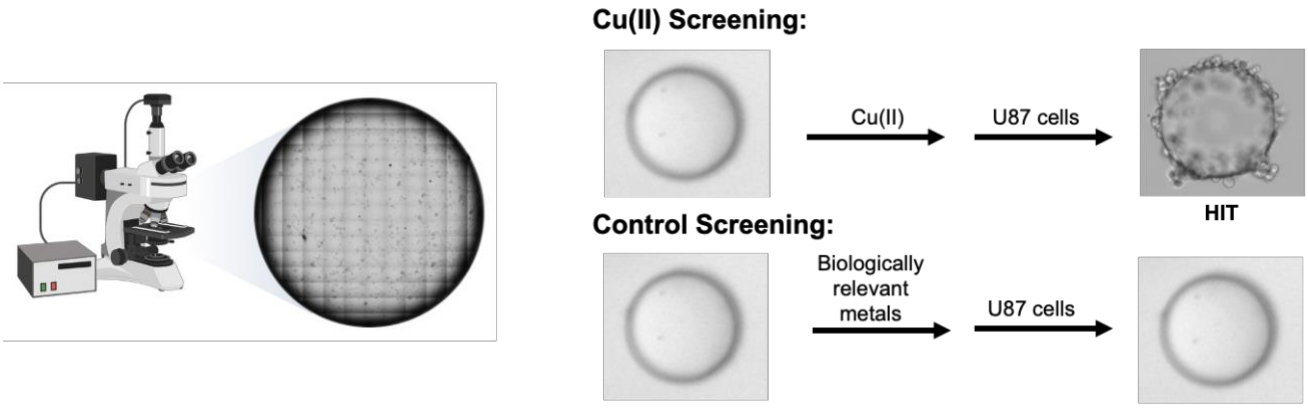

Figure 5. Workflow for screening Cu(II) binding peptides after synthesis of the peptide library. Biologically relevant metals include Zn(II), Fe(II), Mn(II), Na(I), Ca(II), K(I), Mg(II).

The top 5 hits were selected, ranked in terms of strength of hit with Cu(II) and selectivity over the other metals. Beads were placed on porous filter paper, then sequenced by Edman degradation. While some challenges arose with sequencing, one peptide emerged with the sequence Pyr-GRGDdG-Pyr, named Pyr-2, with the non-natural amino acid pyridine at the N- and C- terminus.

To confirm the Pyr-2 sequence was mediating the binding of Cu(II), Pyr-2 was synthesized by solid phase peptide synthesis and purified by high performance liquid chromatography (HPLC). It is vital to ensure that the peptide sequence is a hit off-bead as on-bead, since aggregation or various interactions may affect the binding of the peptide to Cu(II).[38] We applied UV-Vis spectroscopy to assess Cu(II)-binding to pyr-2. The spectrum of Pyr-2 shifts in the presence of Cu(II). The addition of 1 equivalence of Cu(II) to Pyr-2 in HEPES buffer at pH= 7.4 shows λ_{max}=650 nm in comparison to the Pyr-2 alone, which exhibits aw λ_{max} at 650 nm, supports the notion of Cu(II)-binding.

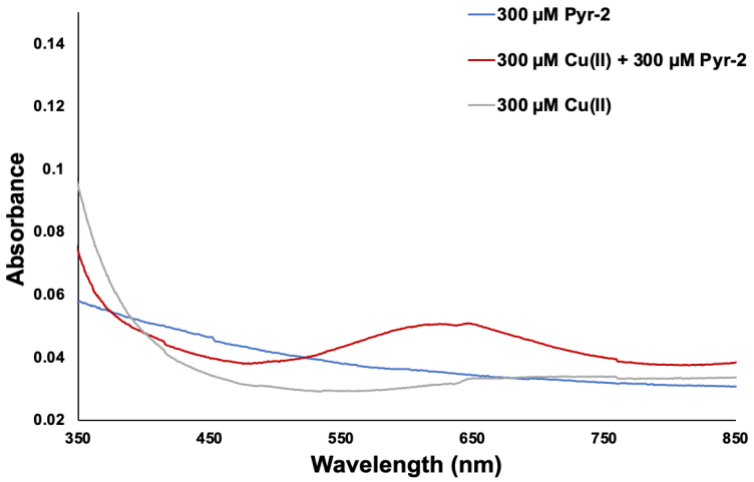

Figure 6. UV-Vis of Pyr-2 in the presence of Cu(II) at 300 µM in MOPS buffer.

2.5 Conclusion

Here, we observed that OBOC could be applied along a cell-based screen to identify peptide sequences with the ability to bind Cu(II) in a way that modulates receptor interactions. The Cu(II)-selectivity of the peptide was identified through the use of multiple on-bead screenings in comparison to other biologically relevant metals. Validation by UV-Vis shows that the top hit, Pyr-2 to be promising. Future work will involve fluorophore conjugation to the peptide alongside cell-based assays with the synthesized probe candidate.

2.6 Materials and Methods

2.6.1 Materials

All chemicals and reagents were purchased from Fisher Scientific, Sigma Aldrich, or Spectrum Chemicals unless otherwise noted. Specifically, dimethylformamide (DMF), 4-methylpiperidine, N,N,N′,N′-tetramethyl-O-(1H-benzotriazol-1-yl)uronium hexafluorophosphate (HBTU), N,N-diisopropylethylamine (DIEA), dichloromethane (DCM), 2,2,2-trifluoroacetic acid (TFA), diethyl ether, methanol, formic acid (FA), $MnCl_2$, $CuCl_2$, 4-(2-hydroxyethyl)-1-piperazineethanesulfonic acid (HEPES), NaOH, HCl, ethylenediaminetetraacetic acid (EDTA), were purchased from ThermoFisher; PEGA resin, $ZnCl_2$ and $FeCl_3$. KCl, and NaCl were purchased from Sigma-Aldrich; and piperidine was purchased from Spectrum Chemicals. Wang resin preloaded with Fmoc-Gln(Trt)-OH, along with Fmoc-protected amino acids were purchased from ThermoFisher but manufactured by ChemImpex. Buffered solutions and metal salt solutions were made using Direct-Q 3 deionized water (>18 MΩ, Millipore). Fmoc-D-Asp(OtBu)-OH is from Millipore.

2.6.2 Building OBOC Library

One gram of PEGA beads were swollen overnight before washing with DMF, methanol, and DMF. The beads were split into 20 different filtered columns labeled with each amino acid. Each amino acid was dissolved with diisopropyldicarbodiimide (DIC) and Oxyma Pure using six equivalence excess and added to each labeled filtered column. The first coupling was shaken overnight. Then after draining the solution and washing with DMF, methanol, and DMF again, the first coupled amino acids were monitored by the Kaiser test (see section 2.4.3). After successful coupling, the beads were pooled together and washed 10x's with DMF, methanol, and

DMF. Fmoc-deprotection was achieved using 20% 4- methylpiperidine in DMF for 15 minutes. For each randomized coupling, the beads would be re-divided and coupled with the next amino acid, DIC, and Oxyma Pure for 15 minutes at 95^{o}C. The beads were then pooled together when coupling the same amino acid (Arg-Gly-Asp in this case), then re-divided at the C-terminus for randomization at this position. Once the sequence was complete, the amino acid side chains were deprotected with a cocktail containing phenol/thioanisole/triisopropylsilane/trifluoroacetic acid (7.5:5:5:5:2.5:82.5 w/v/v/v/v). Then, the beads were drained and washed 10 times with DMF, methanol, and DCM. The beads were dried overnight to evaporate the DCM. The beads were stored in the -20^{o}C freezer. When ready for screenings, the beads were freshly plated onto 6-well plates with water for same day use.

2.6.3 Monitoring Coupling Reaction

The Kaiser test was utilized to confirm the presence or absence of free amine groups with each coupling and deprotection step. The Kaiser test uses three solutions: Reagent A: 1 mL KCN in 49 mL pyridine, Reagent B: 1.0 grams of ninhydrin in 20 mL n-butanol, and Reagent C: 40 g phenol in 20 mL of n-butanol. The general procedure for the test is as follows: 10-15 beads were washed and placed in an Eppendorf tube. Add 2 to 3 drops of each reagent in the Eppendorf tube. Using a heating block, the tube was heated at 110^{o}C for 5 minutes. For successful coupling, beads should be colorless. For successful deprotection, beads are dark blue.

2.6.4. Screening for Peptide Hits

After the peptide library was synthesized, the beads were dried by vacuum in the filtered column and plated in plastic 6-well plates with nanopure water. Screening consists of incubating

the immobilized beads for 30 minutes with 1 μM Cu(II) to ensure Cu(II) interaction with the peptides first followed by a wash with PBS to remove excess Cu(II). Then U87 cells were added to the beads for an additional 30 minutes at 37°C. The beads were washed with PBS, 10 times to remove excess Cu(II) and U87 cells. The beads were then imaged under the EVOS M7000 microscope to observe the hits. The cells were removed via a wash with 7M guanidine for 30 minutes and the metal ion was removed with a 10 mM EDTA wash for one hour. The plated beads were then washed with methanol and reused for control screenings. Once the hits were determined from the screenings, the beads in PBS were viewed under the microscope, then using a p20 pipet, each hit is individually picked from the well and placed on a porous filter paper for sequencing by Edman degradation.

2.6.5 Metal Binding Studies by UV-Vis Spectroscopy

All measurements were recorded on UV-1900 Shimadzu at room temperature with quartz cuvettes with 1 cm path length (Starna Cells). 300 μM of Pyr-2 was dissolved in 50 mM MOPS buffer at pH=7.4 and sonicated for 10 minutes. 300 μM of $CuCl_2$ was dissolved in MilliQ water. Water was used as the spectral reference. In a cuvette, 115 μL of Pyr-2 in MOPS buffer was added and the measurement was recorded. The absorbance for the peptide alone in MOPS buffer was recorded. Then, 115 μL of Cu(II) are added in order to obtain the spectra of 1:1 Cu(II) to Pyr-2.

CHAPTER 3: RATIONAL PEPTIDE DESIGN FOR CU(II) SELECTIVITY

3.1 Introduction

Many probes study intracellular Cu(I), but tend to disregard Cu(II) in the extracellular space.[1,15] This is due to the many challenges associated with develop an extracellular Cu(II) probe including Cu(II) quenching and competition with other metals.[1,15] Therefore, the goal of this chapter is to design, synthesize, and validate the utility of fluorophore labeled peptides for Cu(II) selectivity.

In Chapter 2, we described our efforts to identify a Cu(II)-binding peptide platform via a one-bead-one-compound screening approach. We had utilized a cell-based screen with peptides derived from cyclic integrin-binding peptides that were modified to linear forms. The screen was used to identify peptides that could be conformationally modified by Cu(II) for integrin binding to allow for Cu(II)-dependent interactions with the cell surface. The screen revealed a peptide hit where the cysteines at the N- and C- terminus of the parent linear peptide were replaced with pyridines, N-heterocycles known to coordinate Cu(II).

While the OBOC method is useful in screening a wide variety of sequences, the hits must be validated off-bead as various interactions could interfere with the screen. For instance, a peptide may interact with itself on-bead since each bead in the OBOC peptide library contains 10^{13} copies of the peptide.[34] Due to the intra- and intermolecular forces that may be involved during the screening process between the beads and the iterative copies of each randomized peptide on one bead, there can be false positives when screening for peptides. There may be a high rate of false positive hits or missed hits after synthesis and testing the hits with in vitro assays due to inhomogeneity in a bead population when finding hits through the OBOC screening.[39] Thus, instead of pursuing further screenings by OBOC, we opted to use the hit of the

initial screen as a template for rationally designing fluorophore-conjugated Cu(II)-binding peptides, which is the focus of this chapter. The RGD motif for integrin recognition is maintained in these sequences, but the N- and C- terminus of these peptides have expanded to other Cu(II) binding amino acids.

3.2 Rational Design of Fluorophore-conjugated Peptides for Cu(II)-binding

A series of peptides were synthesized with a fluorophore tag (See Ch. 3.3 for fluorophore selection and conjugation). The peptides were derived off of the Pyr-2 hit with amino acids selected to optimize Cu(II) interactions. Investigations on Cu(II)-binding peptides have revealed common motifs. Albumin, the most abundant protein in plasma transports copper into blood[40]. Albumin contains the amino terminal Cu(II)- and Ni(II) binding (ATCUN) motif, where the nitrogen from the N-terminal imidazole from histidine is necessary to facilitate copper binding (Figure 7A). With these studies, the ATCUN motif has been used in various peptides in order to chelate copper and potentially use this motif for therapeutics.[40] The motif is similarly found in the human tripeptide, Gly-His-Lys (GHK), a well-known peptide for wound healing and anti-aging.[41] Here, Cu(II) ions coordinate through the nitrogen from the imidazole side chain of histidine, another nitrogen from the glycine, and the deprotonated amide nitrogen of the glycine-histidine bond[41] (Figure 7B). Due to the necessity of histidine in the ATCUN motif, histidines were incorporated at the N- and C- terminus in a peptide named MG-His-2 (Table 1).

Aside from histidines, unnatural amino acids have also been shown to increase the diversity, stability, and specificity of peptides for desired targets[28,32]. For example, N-(pyridin-2-ylmethyl)-2-((pyridin-2-ylmethyl)amino)acetamide (DPMGA), a tetradentate ligand, binds Cu(II) at the pyridyl-N's as electron donors, altering the ligand's conformation. This ligand was

used as a metallophore to remove Cu(II) from redox activity when it is bound to the amyloid beta peptide, a peptide involved in Alzheimer's disease.[42] The use of pyridines for Cu(II)-binding is consistent with the top hit from the OBOC screen (Ch. 2). Thus, the fluorophore was conjugated to Pyr-2 to make the peptide named MG-Pyr-2 (Table 2).

Lastly, a derivative where the Cu(II)-binding groups were replaced with a non-binding amino acid, glycine (Gly), was also synthesized peptides to be used as a control peptide with low Cu(II)-binding affinity. This peptide was named MG-Gly-2 (Table 2).

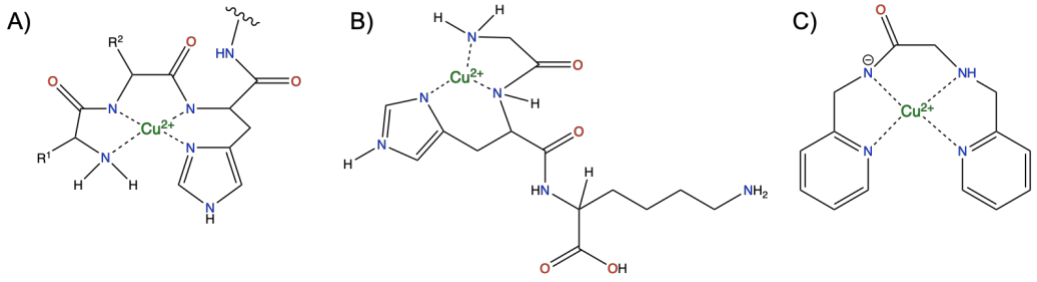

Figure 7. Examples of Copper-Binding peptides. A) GHK tripeptide[41] B) ATCUN motif C) DMPGA, a pyridine containing tetradentate ligand[42]

Name	Sequence	Molecular Weight
MG-Pyr-2	MG-Pyr-GRGDdG-Pyr	1312
MG-His-2	MG-His-GRGDdG-His	1233
MG-Gly-2	MG-Gly-GRGDdG-Gly	1074

Table 2. Peptides discussed in this chapter conjugated to the fluorophore Malachite Green (MG).

3.3 Fluorophore Conjugation to Peptide

In order to monitor peptide localization by fluorescence microscopy, a fluorophore was conjugated to the N-terminus of the rationally designed peptides. Specifically, malachite green, a rotor dye, was chosen as the dye of interest. The use of molecular rotor dyes is advantageous due to its minimal background under a fluorescent microscope, ease of conjugation to peptides, and its increase in fluorescence with restricted rotation or in its "bound state" [43] (Figure 8). Though

there are limited studies imaging cells with molecular rotor dyes, one such study reports the promising use of MG- peptides for imaging live cells as wherein MG fluorescence increases its bound state.[44]

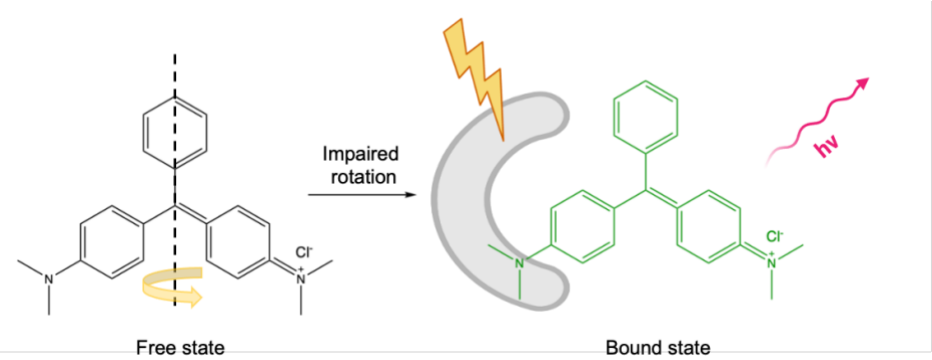

Figure 8. Malachite Green in its free state and bound state.

The MG derivative was synthesized in-house to contain a carboxyethyl terminal group as a synthetic handle for conjugation to the N-terminus of the synthesized peptides by amide coupling. To synthesize this MG synthon, a condensation reaction was performed to form the triphenyl rings followed by oxidation in order to form the active chromophore, carboxyethyl malachite green (Scheme 2). The final product was isolated by flash column chromatography.

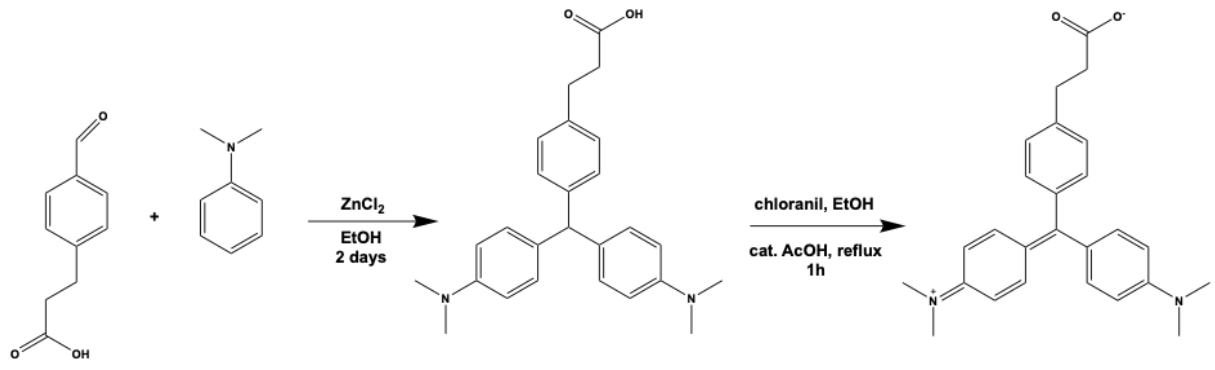

Scheme 2: Carboxyethyl malachite green synthesis[45]

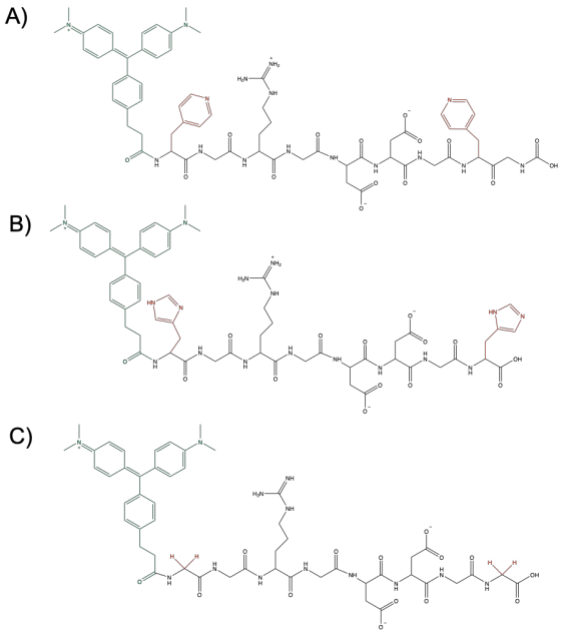

Figure 9. Chemical structure of A) MG-Pyr-2 B) MG-His-2 C) MG-Gly-2.

3.4 Results and Discussion

The peptides listed in Table 2 were synthesized by solid-phase peptide synthesis, with the MG dye installed post-cleavage. Fluorescent cell-based assays were designed and carried out to screen for Cu(II)-mediated binding. We hypothesized that MG-Pyr-2 would exhibit the strongest Cu(II)-responsive effect; thus, MG-Pyr-2 was tested first among the three peptides. MG-Pyr-2 was incubated with various biological metals and U87 cells were added. Fluorescence was measured on a platereader (Figure 10). Surprisingly, when comparing the fluorescence between the control with peptide only and with the various biologically relevant metals, the peptide does not exhibit any selective fluorescence turn-on in the presence of Cu(II) as compared to the other metals. However, a turn-off response was observed with a few metal ions.

To determine whether the turn-off response was due to metal binding, ethylenediamine tetraacetic acid (EDTA) was added. EDTA is a strong chelator for metals ions. With the addition

of EDTA after 30 minutes, the expected observation is a decrease in fluorescence, since copper is no longer mediating peptide binding and integrin recognition. However, after repeating the experiment in triplicate, variable fluorescence is observed.

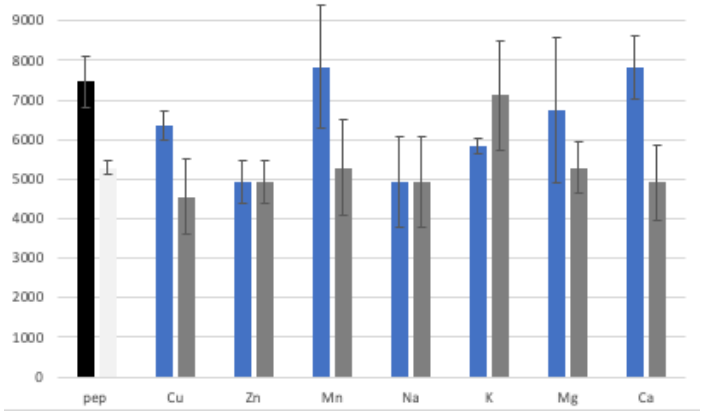

Figure 10. Fluorescence read of MG-Pyr-2 in the presence and absence of biological metals. The blue bar represents the fluorescence due to metal mediated binding with U87 cells. The gray bar represents the fluorescence after addition of EDTA.

At this point, it was uncertain whether the confounding results was due to a systematic error in the experimental design. Thus, fluorescence microscopy was applied in a low-throughput format to assess fluorescence response. The imaging experiment was optimized in terms of the concentration of peptide and Cu(II) to obtain fluorescence signal. A range of 1 to 3 µM of MG-Pyr-2 with 1 equivalent of Cu(II) were tested, finding 3 µM Mg-Pyr-2/Cu(II) as the optimal concentration (Figure 11). Incubation time was also optimized, testing fluorescence response at varying intervals between 15 minutes to two hours of incubation. The results indicated that one hour incubation of the peptide-metal solution with the U87 cells was optimal.

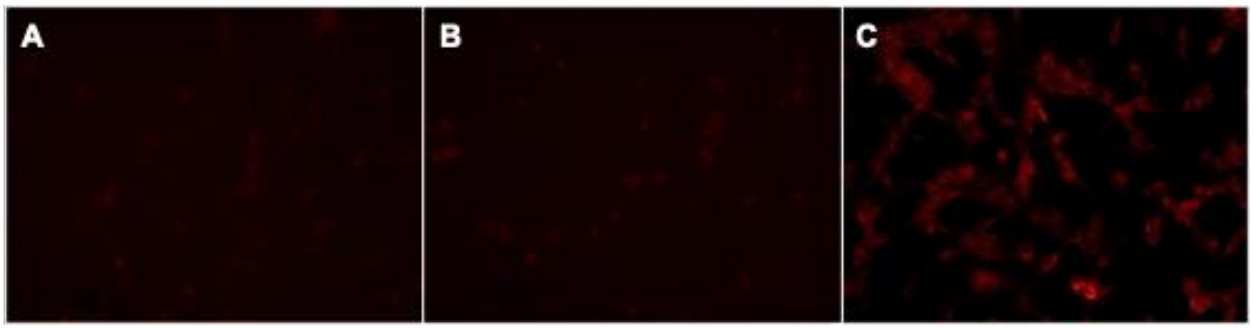

Figure 11. Optimization of peptide to Cu(II) concentration for cell imaging. A) 1 μM Cu(II): 1 μM MG-Pyr-2. B) 2 μM Cu(II): 2 μM MG-Pyr-2 C) 3 μM Cu(II): 3 μM MG-Pyr-2.

These conditions were then applied towards incubation of MG-Pyr-2 with biologically relevant metals (Figure 12). The results remained consistent with the plate reader assays, as MG-Pyr-2 with Cu(II) and other metals did not fluoresce when incubated with U87 cells as compared to the no-metal control. Indeed, the highest fluorescence response was observed with the peptide alone, indicating that the linearization of the peptide may not be sufficient to eradicate binding to the integrins, thus precluding MG-Pyr-2 as a good platform for the target peptide probe.

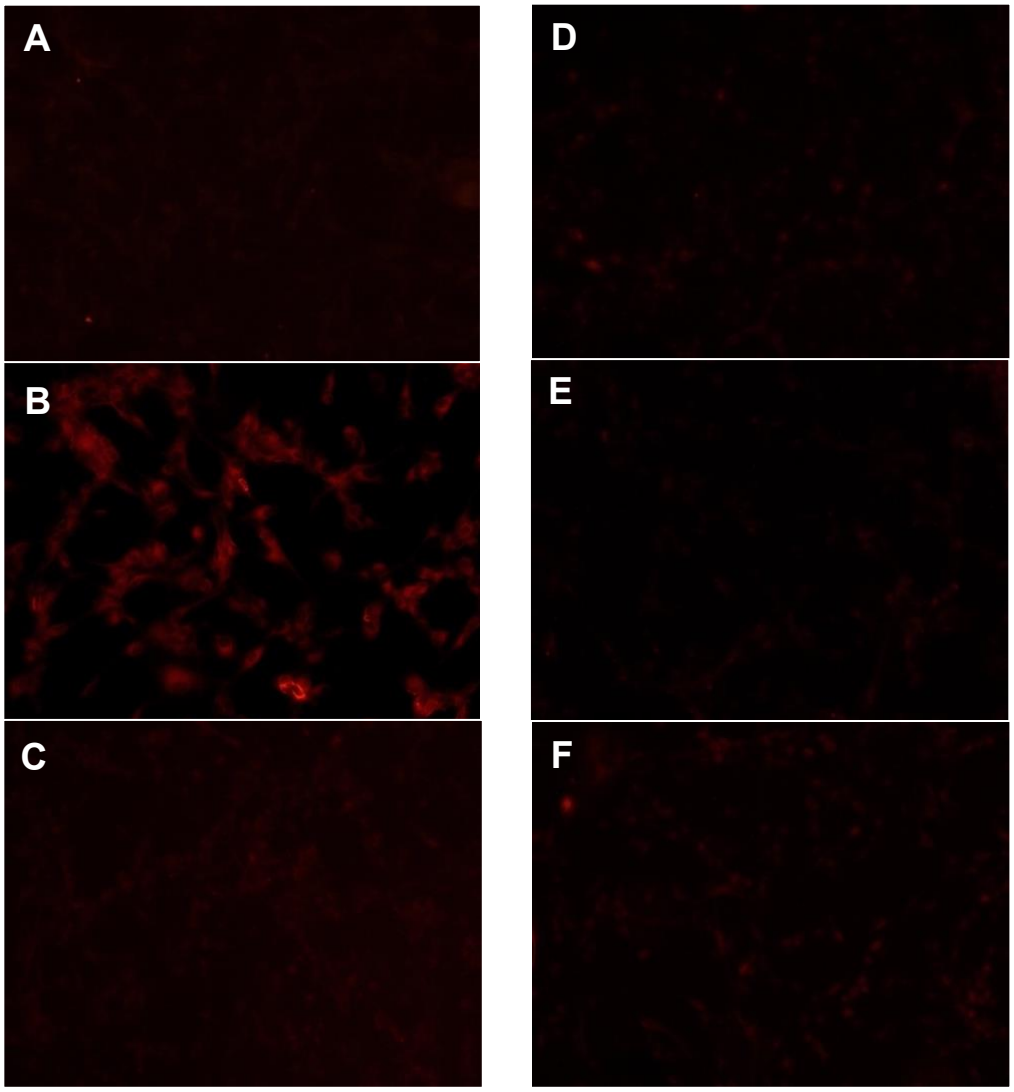

Figure 12. Fluorescence images of U87 cells with A) blank B) MG-Pyr-2 C) Cu(II) + MG-Pyr-2 D) Zn(II) + MG-Pyr-2 E) Mn(II) + MG-Pyr-2 F) Na(I) + MG-Pyr-2.

3.5 Future Work

Although MG-Pyr-2 did not show selective fluorescence for Cu(II) in the cell binding assays, the peptides were successfully synthesized and conjugated to malachite green at the N-terminus of the peptide and validated by mass spectrometry (Section 3.6.4). Future work may include altering the fluorophore position on the peptide. As MG was conjugated close to the N-terminus, it could potentially provide steric hindrances that affect Cu(II) binding. This may be

mitigated by either moving the position of the dye or adding a spacing linker such as polyethylene glycol (PEG) or lysine to distance the dye from the Cu(II)-binding site.

3.6 Materials and Methods

All chemicals and reagents were purchased from the same vendors as above. 3-(4-formylphenyl)propanoic acid and N,N-dimethylaniline were purchased from Fisher Scientific and tetrachloro-1,4-benzoquinone (chloranil) is from Millipore-Sigma.

3.6.1 Cell Culture and Maintenance[46]

Uppsala 87 Malignant Glioma (U87MG) cells were grown in complete DMEM media (Thermo Fisher Scientific) with 10% Avantor Seradigm premium grade fetal bovine serum (FBS), 1 mM sodium pyruvate (Thermo Fisher Scientific), 100 IU penicillin and 100 μg/ml streptomycin (Thermo Fisher Scientific), and 2 mM L-glutamine (Gibco). The cells were subcultured every 2–3 days at 80% confluence. The U87MG cells were gifted to us from Dr. Kit Lam's laboratory. All experiments were performed on cells between passages 10 and 20. Sterile culturing and assay plates were used for the experiments.

3.6.2 Synthesis of Carboxyethyl Malachite Green

Under an inert atmosphere, 1.0 gram of 3-(4-formylphenyl)propanoic acid (5.62 mmol, 1 equivalence) and 1.7 grams of $ZnCl_2$ (12.35 mmol, 2.2 equivalence) were added in 60 mL of anhydrous ethanol. Then, 1.57 mL of N,N-dimethylaniline was added dropwise into the mixture and stirred under reflux overnight. The flask was covered in foil. The solvent was removed by rotary evaporation to yield a leucomalachite green crude mixture. Then, 2.1 grams (8.43 mmol,

1.5 equivalence) of chloranil and a catalytic amount of acetic acid was added to the hot ethanol mixture. This was refluxed for 1 hour. The solution turned dark green. The solvent was removed by rotary evaporation and was purified by flash column chromatography using 6% methanol in DCM to elute impurities, then 10% methanol in DCM to elute the carboxyethyl malachite green product. The purified product was validated by LCMS (400 m/z and UV-Vis absorption at 600 nm).

3.6.3 Solid-phase peptide synthesis of MG-Pyr-2

MG-Pyr-2 (Malachite Green- Pyr- GRGDdG-Pyr) was synthesized manually using standard 9-fluorenylmethoxycarbonyl (Fmoc) solid-phase peptide synthesis (SPPS) methods. For a 0.2 mmol synthesis, Fmoc-Wang resin was first swelled overnight in DMF. Resin was washed 5 times with DMF. The N-terminal was deprotected with 20% 4-methyl-piperidine for 15 minutes shaken. Then, Fmoc-3-(3'-pyridyl)-L-alanine was coupled overnight using diisopropylcarbodiimide (DIC) (4.0 equivalences) and Oxyma Pure (4.0 equivalences) for activation and coupling in DMF. The resin was then washed with DMF 10 times, then deprotected. Amino acids (4.0 equivalences), DIC (4.0 eq.), Oxyma Pure (4.0 eq.) were dissolved in minimal amount of DMF and added to the resin. The resin and amino/acid DIC/Oxyma Pure solution was heated for 20 minutes at 95^{o}C, shaken after 10 minutes, then washed with DMF 10 times. This process was repeated from the deprotection step for each amino acid. After the last amino acid was added, the peptide was washed 10 times with DMF followed by 10 washes with dichloromethane (DCM) and dried overnight. The peptide was coupled to carboxyethyl malachite green by 2-(1H-7-azabenzotriazol-1-yl)-1,1,3,3-tetramethyl uranium hexafluorophosphate and N,N-diisopropylethylenamine for activation and coupling in

DMF overnight at room temperature. The peptide was cleaved from the resin with 95% trifluoroacetic acid, 2.5% triisopropylsilane, and 2.5% H_2O for four hours at room temperature with shaking. The solution was separated from the resin and precipitated in chilled diethyl ether and the suspension was centrifuged at 3900 rpm for 10 minutes at room temperature. The supernatant was decanted and diethyl ether was used for washes after centrifugation. The pellet was dried by vacufuge.

3.6.4 Peptide Purification

Analytical LCMS was performed with H_2O with 0.01% formic acid and acetonitrile (ACN) with 0.01% formic acid in the mobile phase with an Atlantis T3 C18 column to optimize the purification method. An isocratic gradient at 5% ACN for 10 minutes followed by a linear gradient from 5-80% ACN over 37.5 minutes, then an isocratic gradient at 80% ACN for 10 minutes was used with a flow rate of 1 mL/min. Similarly, preparative HPLC was performed for peptide purification with a flow rate of 15 mL/min. On the preparative HPLC, the eluents were monitored by UV-Vis absorption at 220nm for peptide bond absorbance. Peptide purity and identification were characterized by analytical HPLC (t_R= 23.4 minutes) and paired with ESI-MS (m/z = 1311, $m+2H^+/2$= 656). The purified peptide was dried by vacufuge overnight and used for subsequent experiments.

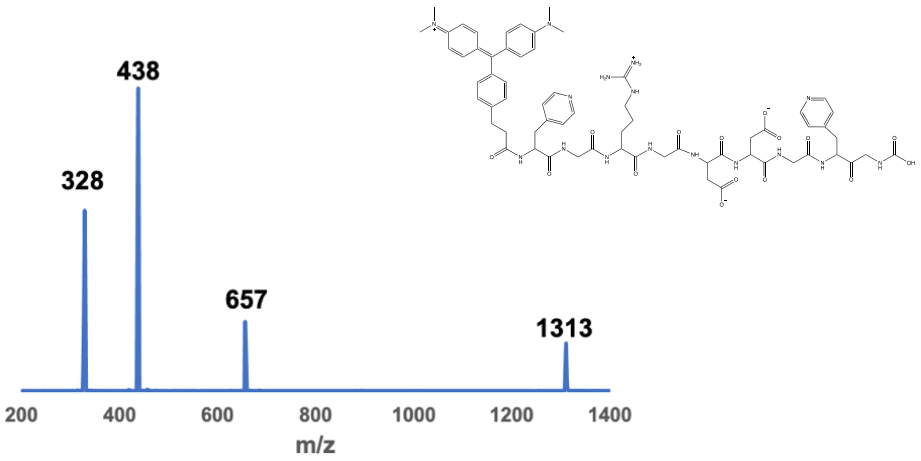

Figure 11. LCMS mass spectrum of purified MG-Pyr-2.

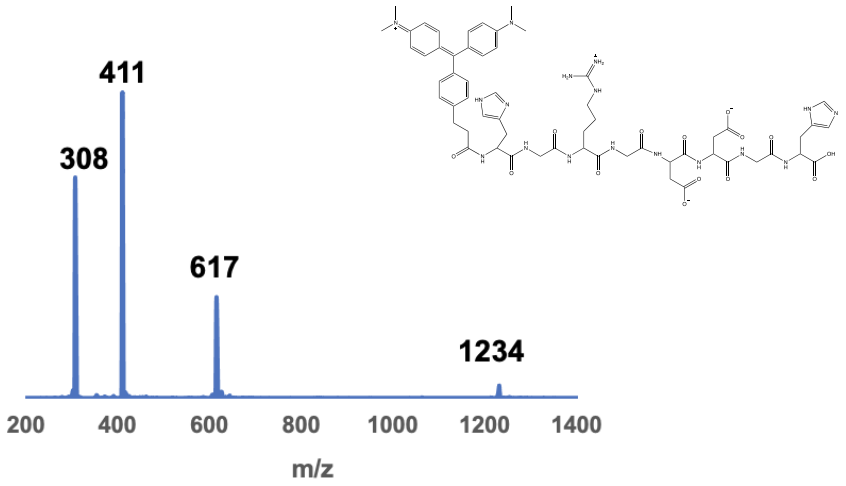

Figure 12. LCMS mass spectrum of MG-His-2.

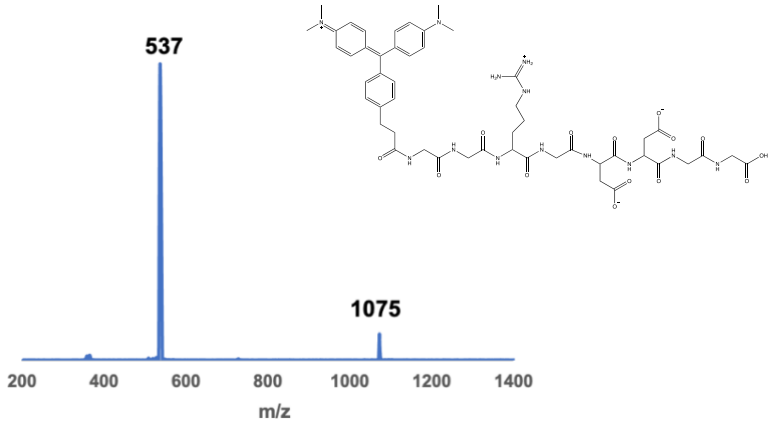

Figure 13. LCMS mass spectrum of MG-Gly-2.

3.6.5 Fluorescence Assays

U87 cells were cultured and plated in a 6-well plate overnight with 20,000 cells per well. The next day, cDMEM is removed from the cells. The cells are washed three times with PBS. Then the cells were placed in media without FBS for fluorescence assays.

3.6.6. Plate Reader

Dissolve 3 μM of MG-Pyr-2 in PBS. Sonicate for 5 minutes. Store in the dark. Prepare 3 μM of $CuCl_2$, $ZnCl_2$, $MnCl_2$, NaCl, $CaCl_2$, KCl dissolved in water. Then, pre-mix 100 μL of peptide with 100 μL of metal for 30 minutes in the dark. U87 cells were trypsinized and added to a 96-well plate and used as a suspension. The plate was incubated in the dark for 1 hour at 37C with shaking. With the plate reader, a well scan was done with shaking between each well for 10 seconds. The fluorescence measurements were read as endpoint measurements at an excitation of 600nm and emission at 650nm, which corresponds to the optical properties of malachite green.

3.7.7 Cell Imaging

In a 12-well plate with acid-washed coverslips, 20,000 U87 cells were plated overnight in cDMEM. The next day, U87 cells were washed with PBS and media without FBS (starvation media). Pre-incubation of 10 μM of Cu(II) and 10 μM of MG-Pyr-2 at 37 ºC in an Eppendorf tube was performed in the dark. Stimulation of cells consisted of addition of the metal-peptide mixture for one hour with no shaking in the dark. After incubation, the cells were washed 10 times with PBS. Then 4% formaldehyde in PBS was added to the stimulated cells for 10 minutes in the dark (covered in foil) at room temperature. After 15 minutes, the fixed cells are washed

with PBS 10 times then sealed onto glass slides overnight in the dark. The next day, the cells were subjected to imaging under a fluorescence microscope.

CHAPTER 4: BIPYRIDINE SYNTHESIS

4.1 Introduction

In Chapter 3, we described our efforts to design a copper-selective integrin-binding fluorescent peptide probe. However, our initial studies showed that the target peptides were not responsive to CuII) within cell systems. This chapter describes efforts to expand our access to unnatural amino acid side chains with enhanced Cu(II) affinity and selectivity. Specifically, we describe synthetic to design a bipyridine-containing amino acid unit. Bipyridines are a good candidate for the design of Cu(II)-binding peptides as these units have been incorporated into other biological polymers to bestow metal binding activity.[28,29] In addition to its potential as a high-affinity Cu(II) ligand, incorporating such an unnatural amino acid unit into a peptide could enhance stability against proteases.[28] Unfortunately, purchasing the unnatural amino acid is prohibitively expensive for incorporating into OBOC-type library syntheses. This chapter describes our efforts to synthesize the bipyridine-alanine unnatural amino acid in large scale based on a previously published method.[28]

The synthesis for the bipyridine unnatural amino acid (Scheme 2) begins with a C-C bond formation through Stille-cross coupling to obtain 5-methyl-2,2'-bipyridine (**3)**. After synthesis of the methyl bipyridine, the methyl group is brominated to obtain 4-(bromomethyl)-2,2'-bipyridine (**4**). In order to proceed to the next step to add the alanine amino acid portion of bipyridine, hydration synthesis is used to obtain a mixture of isomers of product **6**. Then in acidic conditions, the esters on **6** are able to hydrolyze to convert to the bipyridine with a carboxylic acid (**7**). The carboxylic acid is necessary for amide coupling to a peptide. Lastly, the addition of an alkaline protease enzyme is able to preferentially select for the L-bipyridine amino acid isomer over the D-isomer[47].

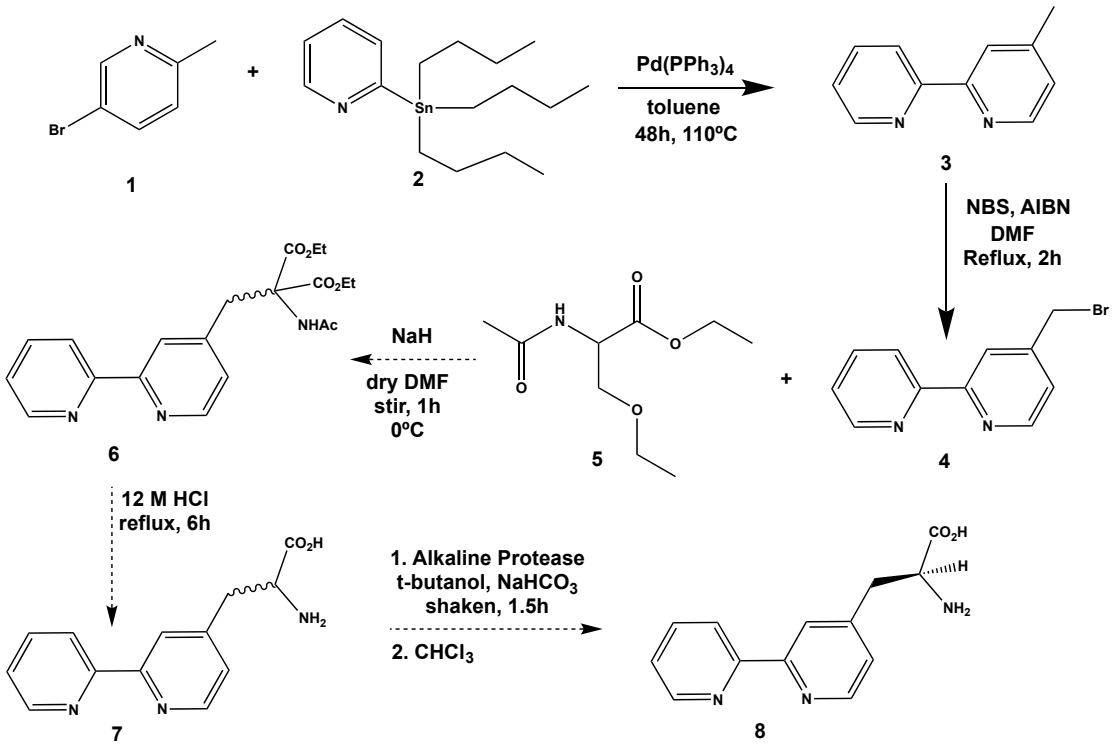

Scheme 2: Synthetic route to the bipyridine alanine unnatural amino acid unit.

4.2 Step 1: Stille Coupling Optimization

The Stille coupling reaction is used for C-C bond formation. Its distinct use of organostannanes and an aryl halide makes it a versatile reaction to use for a variety of functional groups.[48,49] As a typical cross-coupling reaction, the mechanism (Scheme 3) begins with an 18-electron palladium catalyst, in this case, tetrakis(triphenylphosphine)palladium(0), or $Pd(PPh_3)_4$. With ligand dissociation, the palladium catalyst becomes an active 14-electron intermediate, $Pd(PPh_3)_2$. This complex is able to oxidatively add the 2-bromo-5-methylpyridine, resulting in a 16-electron Pd(II) intermediate. Then, with the organostannane, 2-tributylstannylpyridine ($Sn(Bu)_3py$), the reaction goes through transmetalation, where the pyridine is introduced to the Pd(II) complex and the organostannate removes the bromine. From there, the C-C bond

formation occurs in the last step of reductive elimination, returning the catalyst back to a 14-electron Pd(0).

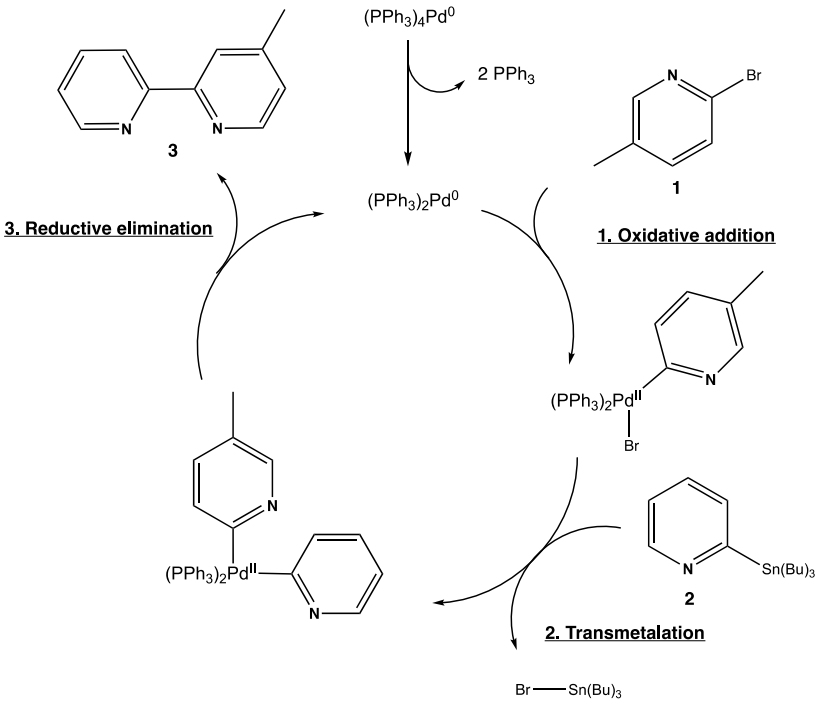

Scheme 3: Stille Coupling Mechanism for 5-methyl-2,2'-bipyridine.

In initial attempts, the Stille cross-coupling step gave low yields, so reaction conditions were optimized. First, increasing equivalences of 2-tributylstannylpyridine ($Sn(Bu)_3py$) were tested to see if the reaction would proceed further. Due to the reactivity of $Sn(Bu)_3py$ towards air and the storage limitations within the laboratory, it may quench easily. $Sn(Bu)_3py$ available in solution may contain some hydrolysis or decomposition by-products, reducing the conversion of bipyridine.[48] On the other hand, the steps taken to form the bipyridine product may also be reversible, so the increased equivalences of $Sn(Bu)_3py$ can reduce the likelihood of reaction reversibility.[48] To ensure successful coupling, increased amounts were used in the first step of the bipyridine synthesis (Table 3, Entry 2 and 3).

As shown in Table 3, Entry 1 were the first conditions used, which was taken from the published protocol. However, conversion was only 25% under these conditions. Increasing equivalences (Entry 2 and 3) showed improved yields. With these encouraging results, the reaction time was then increased and further showed improvements (Entry 4). Thus, the higher equivalents and longer reaction time shown in Entry 4 were applied for this reaction.

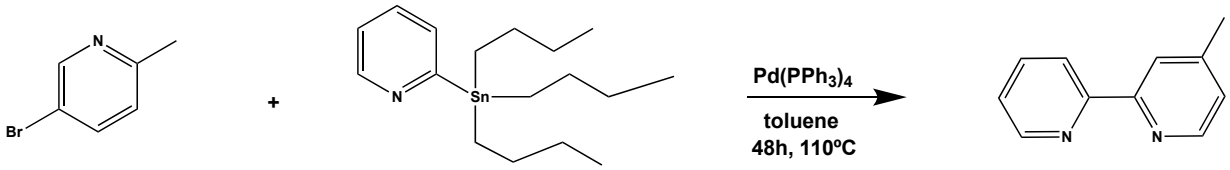

Entry	Bromopyridine eq.	$Sn(Bu)_3py$ eq.	Time	Conversion*
1	1	1	48h	25%
2	1	1.5	48h	30%
3	1	2	48h	92%
4	**1**	**2**	**60h**	**100%**

Table 3. Optimization table for 3-tributylstannylpyridine equivalences.

4.3 Step 2: Bromination of methyl bipyridine

Free radical bromination was previously reported for benzylic bromine substitution to generate **3**. However, I sought to improve its conversion from 40%. Radical bromination by Br_2 results in lower conversions due to unwanted side products generated by Br_2 via electrophilic substitution and dibromination.[50,51] I thus employed the Wohl-Ziegler reaction, which is an N-bromosuccinimide- based benzylic bromination[52]. The first step of the reaction is the initiation step (Scheme 4). It utilizes a radical initiator, azobisisobutyronitrile (AIBN), in order to activate N-bromosuccinimide (NBS). This generates the radical bromine necessary for bromination. Then in the propagation step, the bromine radical is able to remove a benzylic hydrogen. The bipyridine radical intermediate is produced and stabilized by resonance. NBS is then able to

generate bromine for the benzylic substitution of bromine in the termination step, forming the desired product **4** at 87% conversion.

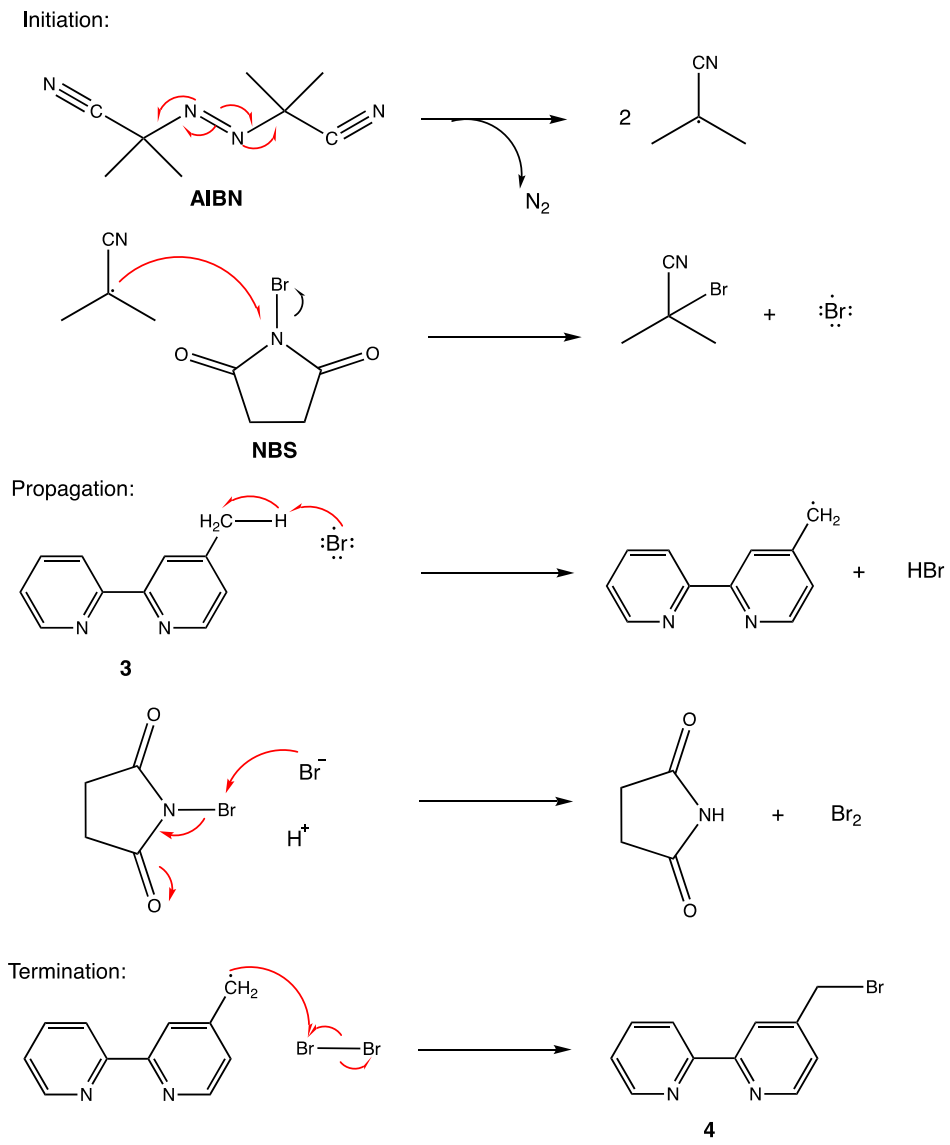

Scheme 4: Wohl Ziegler Bromination of methylbipyridine.

4.4 Results and Conclusions

After optimization and synthesis of 5-methyl-2,2'-bipyridine (**3**) and 4-(bromomethyl)-2,2'-bipyridine (**4**), they were both purified by silica gel flash column chromatography with

yields of 72% and 48%, respectively. The ^{1}H NMR for **3** and **4** (Figure 15, 16) shows successful purification and validation of the desired structures.

Future work includes completing the target synthesis and incorporating the unnatural amino acid into the peptide sequences/library described in Chapters 2 and 3.

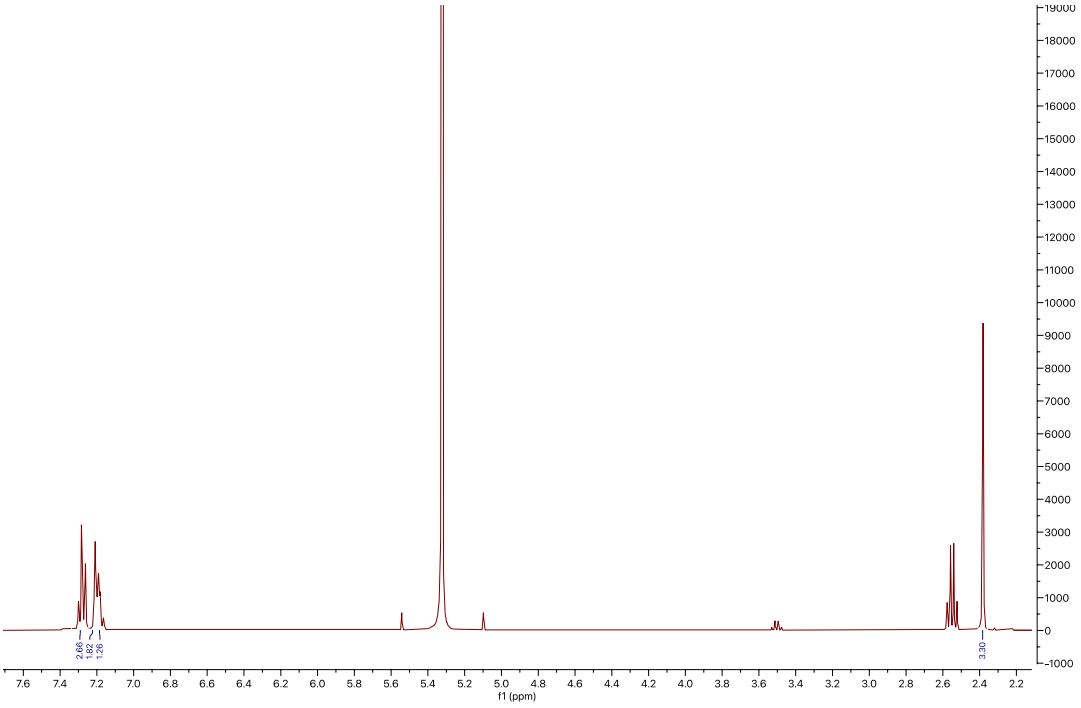

Figure 15. ^{1}H NMR of 5-methyl-2,2'-bipyridine in CD_2Cl_2

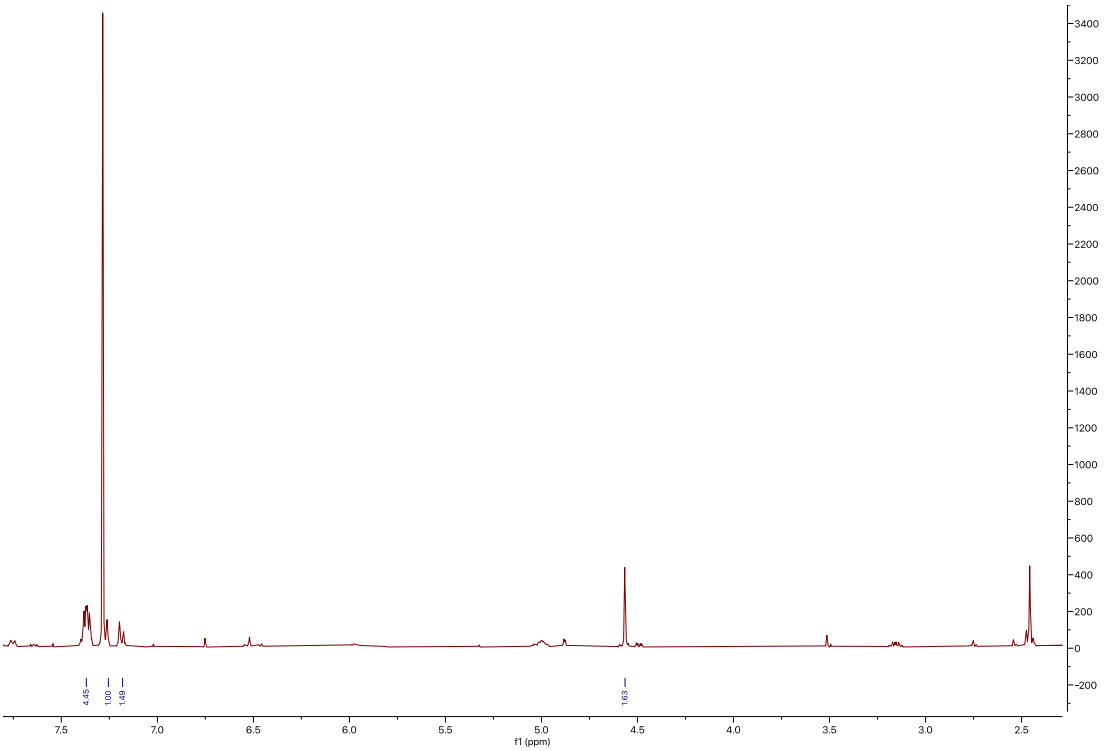

Figure 16. ^{1}H NMR of 4-(bromomethyl)-2,2'-bipyridine (**3**) in $CDCl_3$

4.5 Materials and Methods

All chemicals and reagents were purchased from the same vendors as above. 2-tributylstannylpyridine, 2-bromo-5-methylpyridine, and bromine were purchased from Fisher Scientific.

4.5.1 Stille Cross Coupling of 5-methyl-2,2'-bipyridine

2-bromo-5-methylpyridine (500 mg, 1 eq.) and $Pd(PPh_3)_4$ were added to a round-bottom flask, then the flask was vac and purged three times under nitrogen. Toluene was added and the reaction was stirred. 2-tributystannylpyridine (1.5 mL, 2 eq.) was then added with a syringe dropwise and stirred for 60h at 110°C. The reaction mixture was filtered over Celite and evaporated under pressure (rotavap). The residue was dissolved in EtOAc and washed with

saturated $NaHCO_3$. The organic layer was dried with $MgSO_4$ and concentrated under pressure (Rotavap). 5-methyl-2,2'-bipyridine (**3**) was purified by flash column chromatography with DCM and 1% triethylamine. **3** was evaporated under pressure as a colorless oil. Figure 15 shows the ^1H NMR for the final product with 72% yield. ^1H-NMR (400 MHz, CD_2Cl_2): δ 2.47 (s, 3H), 7.12 (dd, 2H), 7.70 (dd, 2H), 7.87 (m, 3H).

4.5.2 Bromination of 4-methyl-2,2'-bipyridine

3 (25 mg) was added to a round bottom flask with NBS (27 mg, 1 eq.) and AIBN (2.10 mg, 0.085 eq). The flask was vacuum and purged with N_2. 2mL of DMF was added and the reaction was refluxed at 80ºC. The reaction was monitored by TLC for up to two hours. After two hours, DCM was added to a separatory funnel with the reaction mixture. The reaction mixture was washed with water three times and dried over $MgSO_4$. The crude mixture was evaporated under pressure and purified by flash column chromatography with DCM and 0.5% MeOH to isolate 4-methyl-2,2'-bipyridine (**4**). **4** was evaporated under pressure as a white solid. Figure 16 shows the ^1H NMR for the final product with 48% yield. ^1H-NMR (400 MHz, $CDCl_3$): δ 4.53 (s, 2H), 7.14 (dd, 2H), 7.20 (s, 1H), 7.46 (m, 4H).

CHAPTER 5: REDUCED OXYTOCIN

5.1 Introduction

Oxytocin is a well-studied peptide, known as the "love hormone" associated with human physiological processes that include uterine contractions, reproduction, and maternal behavior.[53] Recent research on oxytocin, has shown that the peptide can bind copper and zinc, and that metal interactions may alter its functions.[54] In this chapter, we describe the early stages of adapting oxytocin as a Zn(II)- elective probe as this project aims to utilize reduced oxytocin as a probe for Zn(II).

Previous research shows that Zn(II) binds oxytocin via six carbonyls, forming an octahedral complex[7]. Meanwhile, Cu(II) uses the terminal amine and three deprotonated amides to form a square planar complex.[55] In preliminary work, our lab has observed that metal interactions are distinct between the oxidized cyclic form of oxytocin form (Figure 15A) and the reduced linear form of the peptide (Figure 15B). Specifically, we have observed that Zn(II) can stabilize the linear form to mediate receptor interactions whereas Cu(II) does not have the same effect.

The development of this Zn(II)-responsive platform would provide a tool for scientists to further understand the role Zn(II) may play in both normal and disease states, particularly in extracellular environments of tissues with high expression of the oxytocin receptor.

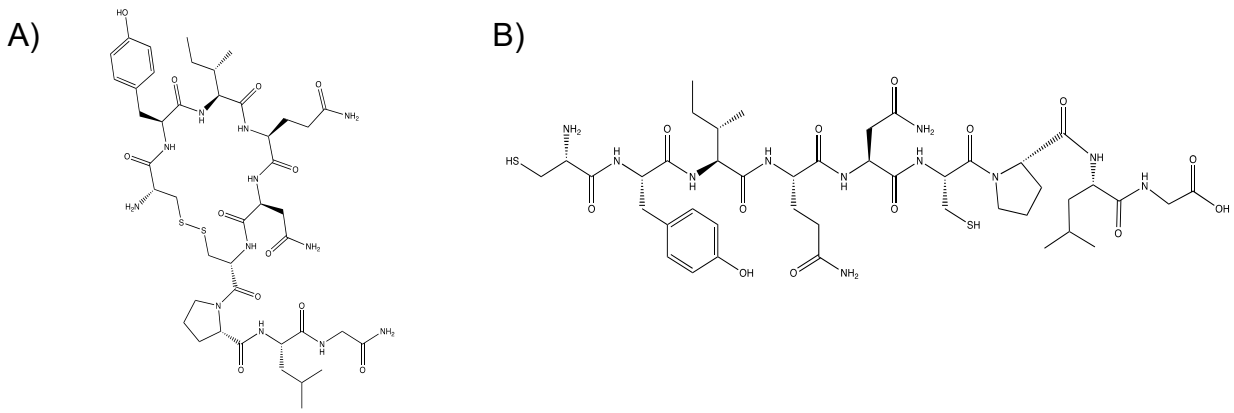

Figure 15. A) Structure of oxytocin (cyclic) B) Structure of reduced oxytocin (linear)

5.2. rOT analogs and FITC conjugation

The first consideration for the design of the oxytocin-based probe is the site at which a fluorophore can be incorporated. Previous research with computational studies, predict that it is necessary for the N-terminus to have a free amine in order to bind with high selectivity for Cu(II). On the other hand, when the N-terminus does not contain a free amine, it is highly selective for Zn(II)[54]. As a result, FITC was conjugated at both the N- and C-terminus of rOT and its analogs (Table 2). FITC-rOT indicates that the fluorophore was conjugated at the N-terminus compared to K-2-FITC indicating the replacement of the tyrosine residue in the oxytocin sequence with a lysine (K) for fluorophore conjugation. Since Zn(II) is does not need tyrosine in order for interaction with oxytocin, it was replaced with Lys(Dde), which has an orthogonal protecting group. Orthogonal protecting groups are advantageous for this design because Dde can be deprotected while the rest of the peptide is protected.[56] This allows for selective on-bead conjugation to FITC after the sequence is synthesized but prior to cleavage.

Peptide	Sequence	Molecular Weight
rOT	CYIQNCPLG	1010
FITC-rOT	FITC-CYIQNCPLG	1399
rOT(K-2-FITC)	CK(FITC)IQNCPLG	1365
FITC-rOT(His-1,6)	FITC-HYIQNHPLG	1468
rOT(K-2-FITC, His-1,6)	HK(FITC)IQNHPLG	1433

Table 2. Reduced OT and analogs sequence and molecular weight.

5.3 Results and Conclusions

After peptide synthesis, the peptides were conjugated to FITC at the N-terminus for FITC-rOT and FITC-rOT(His-1,6) or in place of Tyr for rOT(K-2-FITC) and rOT(K-2-FITC, His-1,6) then validated by LCMS to confirm successful synthesis. For FITC-rOT, the expected m/z is 1400. However, from LCMS, the m/2 was 781, which does not directly correspond to FITC-rOT (Figure 16). This may suggest adduct formation but further analysis of the LCMS data is required to come to this conclusion. Reevaluation of peptide synthesis and conjugation are also currently in progress. One change to consider is the inclusion of DTT to the cleavage cocktail. Peptide cleavage with the addition of DTT ensures that the cysteines in the sequence stay reduced and to avoid disulfide bond formation.

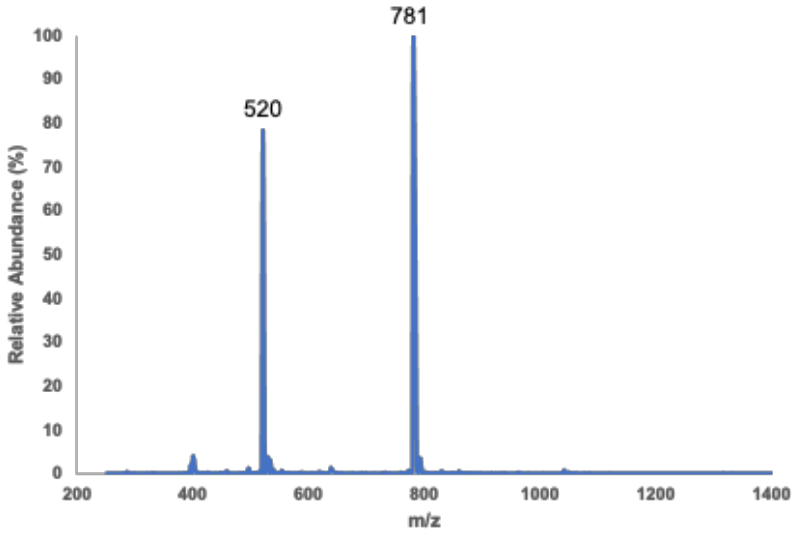

Figure 16. LCMS mass spectrum of rOT coupled to FITC.

5.4 Future Work

To determine whether a given metal ion can selectively bind to these fluorescent rOT peptides, future studies will include assessement by spectroscopic approaches like circular dichroism and electronic absorption. If successful binding is observed, then the rOT peptides can be examined for binding towards the oxytocin receptor in cell lines expressing the receptor, and evaluated via fluorescence imaging.

5.5 Materials and Methods

All chemicals and reagents are purchased from the same vendors listed above. Wang resin preloaded with Fmoc-Gly-OH and Fmoc-Lys(Dde)-OH was purchased from Sigma. Fluorescein isothiocyanate (FITC) was purchased from VWR but manufactured by TCI America. Dithiothreitol (DTT) was purchased from Fisher Scientific.

5.5.1 Synthesis of rOT and analogs

rOT and analogs were synthesized by solid phase peptide synthesis as described in Chapter 3. However, HBTU and DIEA were used as the coupling reagents for this synthesis due as this had shown previous success in the synthesis and purification of the cyclic OT peptide. rOT and analogs were cleaved off the resin with 92.5% TFA, 2.5% TIPS, 2.5% water, 2.5% DTT for 2.5 hours.

5.5.2 Deprotection of Lys(Dde)

After peptide synthesis of the sequence, Lys(Dde) was deprotected by 2% hydrazine in DMF three times for 10 minutes each at room temperature with shaking then washed 10 times with DMF.

5.5.3 FITC Conjugation

If resin was dried, resin was allowed to reswell for one hour in DMF with shaking at room temperature. Then, 2 equivalences of FITC and 6 equivalences of HBTU/ DIEA were added to the resin in DMF overnight at room temperature. The solution was dark yellow for all peptides. After FITC conjugation, peptides were Fmoc-deprotected with 20% 4-methylpiperidine in DMF for 15 minutes.

5.5.4 Peptide Purification of rOT and analogs

Analytical LCMS was performed with H_2O with 0.01% formic acid and acetonitrile (ACN) with 0.01% formic acid in the mobile phase with an Atlantis T3 C18 column. An isocratic gradient at 10% ACN for 10 minutes followed by a linear gradient from 10-50% ACN

over 40 minutes, then an isocratic gradient at 80% ACN for 10 minutes was used with a flow rate of 1 mL/min. Similarly, preparative HPLC was performed for peptide purification with a flow rate of 15 mL/min. On the preparative HPLC, the eluents were monitored by UV-Vis absorption at 220nm for peptide bond absorbance. Peptide purity and identification were characterized by analytical HPLC (t_R= 23.4 minutes) and with LCMS (m/z = 1311, m+2H^+/2= 656). The purified peptide was dried by vacufuge overnight and used for subsequent experiments.

REFERENCES

(1) Dean, K. M.; Qin, Y.; Palmer, A. E. Visualizing Metal Ions in Cells: An Overview of Analytical Techniques, Approaches, and Probes. *Biochimica et Biophysica Acta (BBA) - Molecular Cell Research* **2012**, *1823* (9), 1406–1415. https://doi.org/10.1016/j.bbamcr.2012.04.001.

(2) Crans, D. C.; Kostenkova, K. Open Questions on the Biological Roles of First-Row Transition Metals. *Commun Chem* **2020**, *3* (1), 1–4. https://doi.org/10.1038/s42004-020-00341-w.

(3) Gromadzka, G.; Tarnacka, B.; Flaga, A.; Adamczyk, A. Copper Dyshomeostasis in Neurodegenerative Diseases-Therapeutic Implications. *Int J Mol Sci* **2020**, *21* (23). https://doi.org/10.3390/ijms21239259.

(4) Rivers-Auty, J.; Tapia, V. S.; White, C. S.; Daniels, M. J. D.; Drinkall, S.; Kennedy, P. T.; Spence, H. G.; Yu, S.; Green, J. P.; Hoyle, C.; Cook, J.; Bradley, A.; Mather, A. E.; Peters, R.; Tzeng, T.-C.; Gordon, M. J.; Beattie, J. H.; Brough, D.; Lawrence, C. B. Zinc Status Alters Alzheimer's Disease Progression through NLRP3-Dependent Inflammation. *J. Neurosci.* **2021**, *41* (13), 3025–3038. https://doi.org/10.1523/JNEUROSCI.1980-20.2020.

(5) Wang, F.; Jiao, P.; Qi, M.; Frezza, M.; Dou, Q. P.; Yan, B. Turning Tumor-Promoting Copper into an Anti-Cancer Weapon via High-Throughput Chemistry. *Curr Med Chem* **2010**, *17* (25), 2685–2698.

(6) Li, J. C.; Liu, T.; Wang, Y.; Mehta, A. P.; Schultz, P. G. Enhancing Protein Stability with Genetically Encoded Noncanonical Amino Acids. *J. Am. Chem. Soc.* **2018**, *140* (47), 15997–16000. https://doi.org/10.1021/jacs.8b07157.

(7) Liu, D.; Seuthe, A. B.; Ehrler, O. T.; Zhang, X.; Wyttenbach, T.; Hsu, J. F.; Bowers, M. T. Oxytocin-Receptor Binding: Why Divalent Metals Are Essential. *J. Am. Chem. Soc.* **2005**, *127* (7), 2024–2025. https://doi.org/10.1021/ja046042v.

(8) Gao, J.; Chen, Y.; Guo, Z.; He, W. Recent Endeavors on Molecular Imaging for Mapping Metals in Biology. *Biophys Rep* **2020**, *6* (5), 159–178. https://doi.org/10.1007/s41048-020-00118-7.

(9) Qian, X.; Xu, Z. Fluorescence Imaging of Metal Ions Implicated in Diseases. *Chem. Soc. Rev.* **2015**, *44* (14), 4487–4493. https://doi.org/10.1039/C4CS00292J.

(10) Kardos, J.; Héja, L.; Simon, Á.; Jablonkai, I.; Kovács, R.; Jemnitz, K. Copper Signalling: Causes and Consequences. *Cell Communication and Signaling* **2018**, *16* (1), 71. https://doi.org/10.1186/s12964-018-0277-3.

(11) Chung, C. Y.-S.; Posimo, J. M.; Lee, S.; Tsang, T.; Davis, J. M.; Brady, D. C.; Chang, C. J. Activity-Based Ratiometric FRET Probe Reveals Oncogene-Driven Changes in Labile Copper Pools Induced by Altered Glutathione Metabolism. *Proceedings of the National Academy of Sciences* **2019**, *116* (37), 18285–18294. https://doi.org/10.1073/pnas.1904610116.

(12) Twomey, P. J.; Viljoen, A.; House, I. M.; Reynolds, T. M.; Wierzbicki, A. S. Relationship between Serum Copper, Ceruloplasmin, and Non–Ceruloplasmin-Bound Copper in Routine Clinical Practice. *Clinical Chemistry* **2005**, *51* (8), 1558–1559. https://doi.org/10.1373/clinchem.2005.052688.

(13) Finney, L.; Mandava, S.; Ursos, L.; Zhang, W.; Rodi, D.; Vogt, S.; Legnini, D.; Maser, J.; Ikpatt, F.; Olopade, O. I.; Glesne, D. X-Ray Fluorescence Microscopy Reveals Large-Scale Relocalization and Extracellular Translocation of Cellular Copper during Angiogenesis. *PNAS* **2007**, *104* (7), 2247–2252. https://doi.org/10.1073/pnas.0607238104.

(14) Lutsenko, S. Human Copper Homeostasis: A Network of Interconnected Pathways. *Curr Opin Chem Biol* **2010**, *14* (2), 211–217. https://doi.org/10.1016/j.cbpa.2010.01.003.
(15) Falcone, E.; Okafor, M.; Vitale, N.; Raibaut, L.; Sour, A.; Faller, P. Extracellular Cu2+ Pools and Their Detection: From Current Knowledge to next-Generation Probes. *Coordination Chemistry Reviews* **2021**, *433*, 213727. https://doi.org/10.1016/j.ccr.2020.213727.
(16) Bohrer, D.; do Nascimento, P. C.; Ramirez, A. G.; Mendonça, J. K. A.; De Carvalho, L. M.; Pomblum, S. C. G. Comparison of Ultrafiltration and Solid Phase Extraction for the Separation of Free and Protein-Bound Serum Copper for the Wilson's Disease Diagnosis. *Clinica Chimica Acta* **2004**, *345* (1), 113–121. https://doi.org/10.1016/j.cccn.2004.03.001.
(17) George, T.; Brady, M. F. Ethylenediaminetetraacetic Acid (EDTA). In *StatPearls*; StatPearls Publishing: Treasure Island (FL), 2022.
(18) Poujois, A.; Poupon, J.; Woimant, F. *Chapter 22. Direct Determination of Non-Ceruloplasmin-Bound Copper in Plasma | Elsevier Enhanced Reader*. https://doi.org/10.1016/B978-0-12-810532-0.00022-7.
(19) Solovyev, N.; Ala, A.; Schilsky, M.; Mills, C.; Willis, K.; Harrington, C. F. Biomedical Copper Speciation in Relation to Wilson's Disease Using Strong Anion Exchange Chromatography Coupled to Triple Quadrupole Inductively Coupled Plasma Mass Spectrometry. *Analytica Chimica Acta* **2020**, *1098*, 27–36. https://doi.org/10.1016/j.aca.2019.11.033.
(20) Wieringa, F. T.; Dijkhuizen, M. A.; Fiorentino, M.; Laillou, A.; Berger, J. Determination of Zinc Status in Humans: Which Indicator Should We Use? *Nutrients* **2015**, *7* (5), 3252–3263. https://doi.org/10.3390/nu7053252.
(21) Nolan, E. M.; Lippard, S. J. Small-Molecule Fluorescent Sensors for Investigating Zinc Metalloneurochemistry. *Acc Chem Res* **2009**, *42* (1), 193–203. https://doi.org/10.1021/ar8001409.
(22) Price, T. W.; Firth, G.; Eling, C. J.; Kinnon, M.; Long, N. J.; Sturge, J.; Stasiuk, G. J. A ^{18}F Radiolabelled Zn(II) Sensing Fluorescent Probe. *Chem. Commun.* **2018**, *54* (26), 3227–3230. https://doi.org/10.1039/C8CC00687C.
(23) De Leon-Rodriguez, L.; Lubag, A. J. M.; Sherry, A. D. Imaging Free Zinc Levels in Vivo - What Can Be Learned? *Inorganica Chim Acta* **2012**, *393*, 12–23. https://doi.org/10.1016/j.ica.2012.06.026.
(24) Hennig, G.; Homann, C.; Teksan, I.; Hasbargen, U.; Hasmüller, S.; Holdt, L. M.; Khaled, N.; Sroka, R.; Stauch, T.; Stepp, H.; Vogeser, M.; Brittenham, G. M. Non-Invasive Detection of Iron Deficiency by Fluorescence Measurement of Erythrocyte Zinc Protoporphyrin in the Lip. *Nat Commun* **2016**, *7* (1), 10776. https://doi.org/10.1038/ncomms10776.
(25) Yang, Y.-S.; Ma, C.-M.; Zhang, Y.-P.; Xue, Q.-H.; Ru, J.-X.; Liu, X.-Y.; Guo, H.-C. A Highly Selective "Turn-on" Fluorescent Sensor for Zinc Ion Based on a Cinnamyl Pyrazoline Derivative and Its Imaging in Live Cells. *Anal. Methods* **2018**, *10* (16), 1833–1841. https://doi.org/10.1039/C8AY00037A.
(26) Zastrow, M. L.; Radford, R. J.; Chyan, W.; Anderson, C. T.; Zhang, D. Y.; Loas, A.; Tzounopoulos, T.; Lippard, S. J. Reaction-Based Probes for Imaging Mobile Zinc in Live Cells and Tissues. *ACS Sens.* **2016**, *1* (1), 32–39. https://doi.org/10.1021/acssensors.5b00022.

(27) Lu, Z.; Fan, W.; Lu, Y.; Fan, C.; Zhao, H.; Guo, K.; Chu, W.; Lu, Y. A Highly Sensitive Fluorescent Probe for Bioimaging Zinc Ion in Living Cells and Zebrafish Models. *New J. Chem.* **2018**, *42* (14), 12198–12204. https://doi.org/10.1039/C8NJ02197J.
(28) Liu, C. C.; Mack, A. V.; Tsao, M.-L.; Mills, J. H.; Lee, H. S.; Choe, H.; Farzan, M.; Schultz, P. G.; Smider, V. V. Protein Evolution with an Expanded Genetic Code. *Proceedings of the National Academy of Sciences* **2008**, *105* (46), 17688–17693. https://doi.org/10.1073/pnas.0809543105.
(29) Nisbet, M. L.; Hiralal, E.; Poeppelmeier, K. R. Crystal Structures of Three Copper(II)–2,2′-Bi-pyridine (Bpy) Compounds, [Cu(Bpy)2(H2O)][SiF6]·4H2O, [Cu(Bpy)2(TaF6)2] and [Cu(Bpy)3][TaF6]2 and a Related Coordination Polymer, [Cu(Bpy)(H2O)2SnF6]n. *Acta Crystallogr E Crystallogr Commun* **2021**, *77* (Pt 2), 158–164. https://doi.org/10.1107/S2056989021000633.
(30) Xiao, W.; Li, T.; Bononi, F. C.; Lac, D.; Kekessie, I. A.; Liu, Y.; Sanchez, E.; Mazloom, A.; Ma, A.; Lin, J.; Tran, J.; Yang, K.; Lam, K. S.; Liu, R. Discovery and Characterization of a High-Affinity and High-Specificity Peptide Ligand LXY30 for in Vivo Targeting of A3 Integrin-Expressing Human Tumors. *EJNMMI Res* **2016**, *6*, 18. https://doi.org/10.1186/s13550-016-0165-z.
(31) Humphries, M. J. Integrin Structure. *Biochem Soc Trans* **2000**, *28* (4), 311–339.
(32) Wang, Y.; Xiao, W.; Zhang, Y.; Meza, L.; Tseng, H.; Takada, Y.; Ames, J. B.; Lam, K. S. Optimization of RGD Containing Cyclic Peptides against Avβ3 Integrin. *Mol Cancer Ther* **2016**, *15* (2), 232–240. https://doi.org/10.1158/1535-7163.MCT-15-0544.
(33) Stevenson, M. J.; Farran, I. C.; Uyeda, K. S.; Juan, J. A. S.; Heffern, M. C. Analysis of Metal Effects on C-Peptide Structure and Internalization. *ChemBioChem* **2019**, *20* (19), 2447–2453. https://doi.org/10.1002/cbic.201900172.
(34) Lam, K. S.; Lebl, M.; Krchnˇak, V. The "One-Bead-One-Compound" Combinatorial Library Method. *Chem Rev.* **1997**, 38.
(35) Smith, J. B. Peptide Sequencing by Edman Degradation. In *eLS*; John Wiley & Sons, Ltd, Ed.; Wiley, 2001. https://doi.org/10.1038/npg.els.0002688.
(36) Liu, R.; Enstrom, A. M.; Lam, K. S. Combinatorial Peptide Library Methods for Immunobiology Research. *Experimental Hematology* **2003**, *31* (1), 11–30. https://doi.org/10.1016/S0301-472X(02)01008-1.
(37) *26.7: The Edman Degradation*. Chemistry LibreTexts. https://chem.libretexts.org/Bookshelves/Organic_Chemistry/Organic_Chemistry_(McMurry)/26%3A_Biomolecules-_Amino_Acids_Peptides_and_Proteins/26.07%3A_The_Edman_Degradation (accessed 2022-06-17).
(38) Lam, K. S.; Lehman, A. L.; Song, A.; Doan, N.; Enstrom, A. M.; Maxwell, J.; Liu, R. Synthesis and Screening of "One-Bead One-Compound" Combinatorial Peptide Libraries. In *Methods in Enzymology*; Combinatorial Chemistry, Part B; Academic Press, 2003; Vol. 369, pp 298–322. https://doi.org/10.1016/S0076-6879(03)69017-8.
(39) Doran, T. M.; Gao, Y.; Mendes, K.; Dean, S.; Simanski, S.; Kodadek, T. Utility of Redundant Combinatorial Libraries in Distinguishing High and Low Quality Screening Hits. *ACS Comb Sci* **2014**, *16* (6), 259–270. https://doi.org/10.1021/co500030f.
(40) Harford, C.; Sarkar, B. Amino Terminal Cu(II)- and Ni(II)-Binding (ATCUN) Motif of Proteins and Peptides: Metal Binding, DNA Cleavage, and Other Properties. *Acc. Chem. Res.* **1997**, *30* (3), 123–130. https://doi.org/10.1021/ar9501535.

(41) Pickart, L.; Vasquez-Soltero, J. M.; Margolina, A. The Human Tripeptide GHK-Cu in Prevention of Oxidative Stress and Degenerative Conditions of Aging: Implications for Cognitive Health. *Oxid Med Cell Longev* **2012**, *2012*, 324832. https://doi.org/10.1155/2012/324832.
(42) Jakusch, T.; Hassoon, A. A.; Kiss, T. Characterization of Copper(II) Specific Pyridine Containing Ligands: Potential Metallophores for Alzheimer's Disease Therapy. *Journal of Inorganic Biochemistry* **2022**, *228*, 111692. https://doi.org/10.1016/j.jinorgbio.2021.111692.
(43) Xu, S.; Hu, H.-Y. Fluorogen-Activating Proteins: Beyond Classical Fluorescent Proteins. *Acta Pharmaceutica Sinica B* **2018**, *8* (3), 339–348. https://doi.org/10.1016/j.apsb.2018.02.001.
(44) *Red Fluorescent Turn-On Ligands for Imaging and Quantifying G Protein-Coupled Receptors in Living Cells - Karpenko - 2014 - ChemBioChem - Wiley Online Library*. https://chemistry-europe.onlinelibrary.wiley.com/doi/epdf/10.1002/cbic.201300738?saml_referrer (accessed 2022-06-30).
(45) Jafari, S.; Thillier, Y.; Ajena, Y. H.; Shorty, D.; Li, J.; Huynh, J. S.; Pan, B. M.-C.; Pan, T.; Lam, K. S.; Liu, R. Rapid Discovery of Illuminating Peptides for Instant Detection of Opioids in Blood and Body Fluids. *Molecules* **2019**, *24* (9), 1813. https://doi.org/10.3390/molecules24091813.
(46) Harder, N. H. O.; Lee, H. P.; Flood, V. J.; San Juan, J. A.; Gillette, S. K.; Heffern, M. C. Fatty Acid Uptake in Liver Hepatocytes Induces Relocalization and Sequestration of Intracellular Copper. *Frontiers in Molecular Biosciences* **2022**, *9*.
(47) Feng, Z.; Xu, B. Inspiration from the Mirror: D-Amino Acid Containing Peptides in Biomedical Approaches. *Biomol Concepts* **2016**, *7* (3), 179–187. https://doi.org/10.1515/bmc-2015-0035.
(48) Cordovilla, C.; Bartolomé, C.; Martínez-Ilarduya, J. M.; Espinet, P. The Stille Reaction, 38 Years Later. *ACS Catal.* **2015**, *5* (5), 3040–3053. https://doi.org/10.1021/acscatal.5b00448.
(49) *Stille Coupling*. Chemistry LibreTexts. https://chem.libretexts.org/Bookshelves/Inorganic_Chemistry/Supplemental_Modules_and_Websites_(Inorganic_Chemistry)/Catalysis/Catalyst_Examples/Stille_Coupling (accessed 2022-09-21).
(50) Djerassi, Carl. Brominations with *N* -Bromosuccinimide and Related Compounds. The Wohl-Ziegler Reaction. *Chem. Rev.* **1948**, *43* (2), 271–317. https://doi.org/10.1021/cr60135a004.
(51) Marcos, C. F.; Neo, A. G.; Díaz, J.; Martínez-Caballero, S. A Safe and Green Benzylic Radical Bromination Experiment. *Journal of Chemical Education* **2020**. https://doi.org/10.1021/acs.jchemed.9b00020.
(52) 10.3 Allylic and Benzylic Bromination with NBS. *Chad's Prep®*.
(53) Kotynia, A.; Czyżnikowska, Ż.; Cebrat, M.; Jaremko, Ł.; Gładysz, O.; Jaremko, M.; Marciniak, A.; Brasuń, J. The Role of Hydroxyl Group of Tyrosine in Copper(II) Binding by His-Analogs of Oxytocin. *Inorganica Chimica Acta* **2013**, *396*, 40–48. https://doi.org/10.1016/j.ica.2012.09.035.
(54) Mervinetsky, E.; Alshanski, I.; Tadi, K. K.; Dianat, A.; Buchwald, J.; Gutierrez, R.; Cuniberti, G.; Hurevich, M.; Yitzchaik, S. A Zinc Selective Oxytocin Based Biosensor. *J. Mater. Chem. B* **2019**, *8* (1), 155–160. https://doi.org/10.1039/C9TB01932D.

(55) Joly, L.; Antoine, R.; Albrieux, F.; Ballivian, R.; Broyer, M.; Chirot, F.; Lemoine, J.; Dugourd, P.; Greco, C.; Mitrić, R.; Bonačić-Koutecký, V. Optical and Structural Properties of Copper−Oxytocin Dications in the Gas Phase. *J. Phys. Chem. B* **2009**, *113* (32), 11293–11300. https://doi.org/10.1021/jp9037478.
(56) Conda-Sheridan, M.; Krishnaiah, M. *Protecting Groups in Peptide Synthesis | Springer Nature Experiments*. https://experiments.springernature.com/articles/10.1007/978-1-0716-0227-0_7 (accessed 2022-09-22).